eScholarship

Title

The combinatorics of a tree-like functional equation for connected chord diagrams

Permalink

https://escholarship.org/uc/item/1qg5647z

Journal

ISSN

Author

Nabergall, Lukas

Publication Date

2023

DOI

Supplemental Material

https://escholarship.org/uc/item/1qg5647z#supplemental

Copyright Information

Peer reviewed

THE COMBINATORICS OF A TREE-LIKE FUNCTIONAL EQUATION FOR CONNECTED CHORD DIAGRAMS

Lukas Nabergall[1]

[1]*Department of Combinatorics and Optimization, University of Waterloo, Ontario, Canada.*
lnaberga@uwaterloo.ca

Abstract. We build on recent work of Yeats, Courtiel, and others involving connected chord diagrams. We first derive from a Hopf-algebraic foundation a class of tree-like functional equations and prove that they are solved by weighted generating functions of two different subsets of weighted connected chord diagrams: arbitrary diagrams and diagrams forbidding so-called top cycle subdiagrams. These equations generalize the classic specification for increasing ordered trees and their solution uses a novel decomposition, simplifying and generalizing previous results. The resulting tree perspective on chord diagrams leads to new enumerative insights through the study of novel diagram classes. We present a recursive bijection between connected top-cycle-free diagrams with n chords and triangulations of a disk with $n + 1$ vertices, thereby counting the former. This connects to combinatorial maps, Catalan intervals, and uniquely sorted permutations, leading to new conjectured bijective relationships between diagram classes defined by forbidding graphical subdiagrams and imposing connectedness properties and a rich variety of other combinatorial objects. We conclude by exhibiting and studying a direct bijection between diagrams of size n with a single terminal chord and diagrams of size $n - 1$.

Keywords. Chord diagrams, perfect matchings, combinatorial classes, pattern avoidance, combinatorial maps, triangulations, Catalan posets, uniquely sorted permutations

Mathematics Subject Classifications. 05A05, 05A10, 05A15, 05A18, 05A19

1. Introduction

A chord diagram of size n is a perfect matching of $\{1, 2, \ldots, 2n\}$. Such objects have also been called matchings [Jel07, CDD$^+$07], complete pairings [Ste78], and interval systems [DM21], and can be viewed as set partitions with every block of size 2; see Figure 3.1. Here chord diagrams are rooted at the chord containing 1, but the term has also been used to refer to the unrooted object obtained after modding out by cyclic permutations of $[2n]$. For brevity, we will use the shortened 'diagram' to refer to chord diagrams. There are $(2n - 1)!!$ diagrams of

size n. Other objects counted by double factorials include double occurrence words, fixed-point-free involutions, increasing ordered trees, and Stirling permutations. In the literature, chord diagrams seem to have been first studied by Touchard [Tou52]. Since then there has been much focus on the enumeration of various subclasses of diagrams and their statistics (e.g. [Rio75, Ste78, SE78, NW79, FN00, PR14, CYZ19]). One of the most prominent and natural types of diagrams studied are connected diagrams, which are those diagrams C for which there is no proper interval of $[2n]$ that is the ground set of a subdiagram of C. Connectivity can also be defined via the intersection graph $G(C)$ of a diagram C, the directed graph on the chords of C formed by adding edge (c, c') if c' crosses c on the right; C is connected if and only if its intersection graph is weakly connected. Undirected intersection graphs of diagrams, known as circle graphs, have been studied as pure graph objects (e.g. [Naj85, DM21]) and in particular play a major role in vertex minor theory [Bou94].

Outside of enumerative combinatorics and graph theory, chord diagrams have also appeared in diverse areas such as knot theory [BR00], bioinformatics [HSS98] and, most relevantly for the present purposes, physics [Mah22]. In 2013, Nicolas Marie and Karen Yeats [MY13] solved a certain Dyson–Schwinger equation from quantum field theory. This equation has a recursive form similar to standard functional equations for rooted trees. The solution of Marie and Yeats came as a series expansion indexed by connected diagrams and weighted by coefficients indexed by certain novel parameters of those diagrams. These parameters are the number of terminal chords of a diagram C and their indices under a specific total order on the chords of C, the intersection order; a chord $c \in C$ is terminal if it has no outgoing edges in $G(C)$, that is, if there are no chords crossing it to the right. The intersection order is a natural total order, distinct from the standard ordering of the chords by their first endpoints or sources, that extends the partial order on the chords defined by reachability in the intersection graph. See Section 3 for more details. Following Marie and Yeats, Courtiel and Yeats [CY17, CY19] further studied the expansion over connected diagrams and the associated terminal chords, in particular obtaining probabilistic and asymptotic information about the distribution of the latter. In a different direction, Courtiel, Yeats, and Zeilberger [CYZ19] linked these objects and parameters to combinatorial maps, another well-studied structure. We will further describe related work throughout the paper.

We aim to bring these new equations, parameters, and associated results further into the enumerative combinatorial context and, through this, obtain new insights. In particular, much of this paper can be viewed as illuminating the tree-like structure of chord diagrams and its interplay with notions of connectedness, as well as relating these insights to other combinatorial objects. We begin in Section 2 by showing how generalizations of the Dyson–Schwinger equation considered by Marie and Yeats arise from Hopf subalgebras of the Connes–Kreimer Hopf algebra of rooted trees via a result due to Loïc Foissy [Foi08, Foi10, Foi14]. These equations have the form

$$G(x, y) = xL(\phi(G(x, y))), \tag{1.1}$$

where ϕ is a formal power series with nonzero constant term. The map L is a type of linear map on polynomials in y from cohomology theory known as a *Hochschild 1-cocycle*, or simply *1-cocycle*. There are two such 1-cocyles corresponding to the two coalgebras on the ring of one-variable polynomials, the binomial coalgebra and the divided power coalgebra, leading to

two forms of equation (1.1). Since in the binomial case L generalizes the integral operator, (1.1) generalizes the classic functional equation for the exponential generating function of increasing trees (see e.g. [BFS92]), leading to the term *tree-like* to describe such equations (matching the traditional meaning of the term [BLL98]).

Marie and Yeats [MY13] solved the tree-like equation with L a binomial 1-cocycle and $\phi(z) = 1/(1-z)$. Their solution method proceeded in two steps. First they applied a decomposition on connected diagrams to prove that the solution satisfies a certain recurrence, in the form of a differential equation, which allows them to reduce the problem to verifying the linear term in y. Then they inductively expanded the reduced form of (1.1) to obtain a second recurrence characterizing the solution and proved that it holds by passing through a bijection between connected diagrams and a recursively-defined class of labeled binary trees. Their proof method is quite technical and therefore difficult to understand intuitively and generalize. In Sections 3 through 5 we present a simpler, more direct proof of our main result, Theorem 5.1, generalizing the work of Marie and Yeats, that the binomial and divided power tree-like equations are solved by weighted generating functions for sets of connected chord diagrams. Along the way, in Section 3, we define chord diagrams and their relevant properties and parameters, including the intersection order, terminal chords, and 1-terminality, a property that we show can be viewed as a stronger, ordered form of connectivity. Our proof of Theorem 5.1 works entirely at the level of chord diagrams and is based on a relatively simple decomposition of a connected diagram into "shuffled" connected subdiagrams. This decomposition naturally involves distinguished 1-terminal subdiagrams, beginning to highlight the importance of 1-terminality; in particular, these 1-terminal subdiagrams essentially reveal the underlying tree-like structure of chord diagrams.

The solution to the divided power tree-like equation is indexed by a subset of connected diagrams, namely, those that forbid so-called top cycle subdiagrams, one of only two types of chord diagrams whose undirected intersection graph is isomorphic to a cycle. In Section 6 we describe the bijective relationship between connected top-cycle-free diagrams and planar bridgeless maps discovered by Courtiel, Yeats, and Zeilberger [CYZ19]. This left open the goal, further motivated by our generating function results, of obtaining explicit formulas counting such diagrams. We derive such a formula counting the number of connected top-cycle-free diagrams of size n by constructing an explicit, recursive bijection to triangulations of a disk and applying the work of Brown [Bro64] enumerating these classic objects. This formula is in fact further refined by the index of the first terminal chord in the intersection order, which turns out to correspond to one less than the number of exterior (or boundary) vertices of the triangulation. Alongside prior work by Jelínek [Jel07], these results motivate considering other classes of diagrams determined by forbidding a fixed set of graphically-defined subdiagrams, in the vein of the large body of prior work on analogous classes of graphs as well as pattern-avoiding permutations. In the concluding Section 8 we discuss relationships, both conjectured and proven, between top-cycle-free, triangle-free, tree, chordal, bipartite, and bottom-cycle-free diagrams, where a bottom cycle is the second diagram realizer of a cycle, and intervals of Catalan lattices, uniquely sorted permutations, and a variety of combinatorially-significant number sequences found on the OEIS [SI22]. These relationships in particular appear when the diagrams are required to be connected or 1-terminal, further underscoring the role of connectivity notions. Resolving the

number of conjectures introduced here is a significant line of inquiry for future work, recently begun in [Nab22].

Courtiel and Yeats [CY17] proved that there are $(2n-3)!!$ 1-terminal diagrams of size n, indicating that such diagrams should be in one-to-one correspondence with diagrams of size $n-1$. In the penultimate section of this paper we present a new simple formulation of an unpublished bijection between these two sets first discovered by Yeats. This map ψ is easy to understand structurally. It also has a straightforward relationship with k-terminality, a generalization of 1-terminality analogous to k-connectivity; ψ induces a bijection between k-terminal diagrams of size n and $(k-1)$-terminal diagrams of size $n-1$. Together with a characterization of 1-terminal top-cycle-free diagrams, it follows from this that such diagrams are in bijection with noncrossing diagrams of size $n-1$, so they are counted by the Catalan numbers. We also show that ψ interfaces equally well with nonnesting diagrams, another classic Catalan object. We conclude the section by discussing the action of ψ on other double factorial objects.

Finally, we wrap up the concluding section with a number of open questions for future work.

2. Tree-like equations from the Connes–Kreimer Hopf algebra

First appearing under the guise of the Butcher group in numerical analysis and independently introduced by Kreimer [Kre98] in the context of renormalization in perturbative quantum field theory, the Connes–Kreimer Hopf algebra of rooted trees $\mathcal{H}_{CK}$ is the free associative commutative algebra freely generated over a field K of characteristic zero by the set of rooted trees. As implied, the product is given on the basis of forests of rooted trees by concatenation while the coproduct is defined by setting

$$\Delta(t) = \sum_{\substack{C \subseteq V(t) \\ C \text{ antichain}}} \left(\prod_{v \in C} t_v \right) \otimes \left(t \setminus \prod_{v \in C} t_v \right)$$

for a rooted tree t, where t_v is the subtree of t rooted at v and parent-child is the cover relation for a tree poset, and extending it as an algebra homomorphism to all of $\mathcal{H}_{CK}$; note that here we take $t \setminus t = 1$. From a pure algebraic perspective, the Connes–Kreimer Hopf algebra is important because it possesses a certain *universal property* unique up to isomorphism among Hopf algebras. Let B_+ be the algebra homomorphism attaching a set of rooted trees as children to a new common root. Note that the B_+ operator is a *Hochschild 1-cocycle*, a linear map L such that

$$(\text{id} \otimes L) \circ \Delta + L \otimes 1 = \Delta \circ L.$$

Then the universal property is the following.

Theorem 2.1 (Connes–Kreimer [CK98, Theorem 2]). *Let A be an associative commutative algebra over K and $L \colon A \to A$ be a linear map. Then there exists a unique algebra homomorphism $\rho_L \colon \mathcal{H}_{CK} \to A$ such that $\rho_L \circ B_+ = L \circ \rho_L$. Furthermore, if A is a bialgebra and L is a Hochschild 1-cocycle then ρ_L is a bialgebra homomorphism, and if A is also a Hopf algebra then ρ_L is a Hopf algebra homomorphism.*

There has been considerable interest in understanding Hopf subalgebras of $\mathcal{H}_{CK}$ (see e.g. [Rot15, Dug19]). In a series of papers [Foi08, Foi10, Foi14], Foissy examined subalgebras of $\mathcal{H}_{CK}$ generated by a family of recursive equations, so-called *combinatorial Dyson–Schwinger equations*, of the form

$$T(x) = xB_+(\phi(T(x))) \tag{2.1}$$

for $\phi(z) \in K[[z]]$ with $\phi(0) = 1$. The unique solution to this equation is a formal power series $T(x)$ whose coefficients lie in $\mathcal{H}_{CK}$. Writing $t_n = [x^n]T(x)$, Foissy characterized when the subalgebra $A = K[t_1, t_2, \ldots]$ of $\mathcal{H}_{CK}$ is Hopf.

Theorem 2.2 (Foissy [Foi08]). *A is a Hopf subalgebra if and only if $\phi(z) = (1 + abz)^{-1/b}$ for some $a, b \in K$ with $b \neq 0$ or $\phi(z) = e^{az}$.*

We are interested in equations which arise from (2.1) by applying the universal property to the polynomial algebra $K[y]$ and a linear map $L\colon K[y] \to K[y]$. Applying the algebra homomorphism ρ_L guaranteed by Theorem 2.1 to both sides of (2.1), we get the bivariate *tree-like equation*

$$G(x, y) = xL(\phi(G(x, y))), \tag{2.2}$$

where $G(x, y) = \rho_L(T(x))$. The maps L and ρ_L act on the coefficients in x of $\phi(G(x, y))$ and $T(x)$ term by term additively; since L sends polynomials to polynomials this equation has an inductively specified solution in $K[y][[x]]$, so it is well-formed. In the physics setting, ρ_L corresponds to the Feynman rules which map each Feynman graph to its associated Feynman integral (for details see e.g. [Pan11]). We will be most interested in Equation (2.2) with ϕ set to generate a Hopf subalgebra of $\mathcal{H}_{CK}$ via Theorem 2.2, but will work in the more general setting with ϕ an arbitrary formal power series with constant term 1.

In order to get meaningful combinatorial solutions to (2.2), it is clearly necessary to restrict L to some specific class of linear maps. With that in mind, the universal property points the way towards which classes of maps would be of most interest: Hochschild 1-cocycle operators arising from coalgebra structures on $K[y]$. There are two graded coalgebras on one-variable polynomials classically studied in the literature, namely, the binomial coalgebra and the divided power coalgebra. For the former, the coproduct is defined by setting

$$\Delta(y^n) = \sum_{k=0}^{n} \binom{n}{k} y^k \otimes y^{n-k}.$$

Combining this with the polynomial algebra on $K[y]$ with the usual product, we in fact get a Hopf algebra. The following lemma describes Hochschild 1-cocycles in the binomial coalgebra.

Lemma 2.3. *A map L is a 1-cocycle operator for the binomial coalgebra on $K[y]$ if and only if*

$$L(y^n) = \int_0^y F\left(\frac{d}{dt}\right) t^n dt$$

for some power series $F(z) = \sum_{i \geqslant 0} f_i z^i$ in $K[[z]]$.

Proof. Writing $c_{m,n} = [y^{n-m}]L(y^n)$ for $m \leqslant n$, define

$$L_m(y^n) = \begin{cases} c_{m,n}y^{n-m} & \text{if } n \geqslant m, \\ 0 & \text{else.} \end{cases}$$

Fix $m \leqslant n$ and note that L_m is a 1-cocycle by linearity. Then

$$((\mathrm{id} \otimes L_m) \circ \Delta + L_m \otimes 1)(y^n) = (\mathrm{id} \otimes L_m)\left(\sum_{k=0}^{n} \binom{n}{k} y^k \otimes y^{n-k}\right) + L_m(y^n) \otimes 1$$

$$= \sum_{k=0}^{n} c_{m,n-k}\binom{n}{k} y^k \otimes y^{n-m-k} + c_{m,n}y^{n-m} \otimes 1,$$

while

$$(\Delta \circ L_m)(y^n) = c_{m,n}\Delta(y^{n-m}) = \sum_{i=0}^{n-m} c_{m,n}\binom{n-m}{i} y^i \otimes y^{n-m-i}.$$

Applying the 1-cocycle property and comparing terms, we see that $m \geqslant -1$ since otherwise $x^{n+1} \otimes x^{-m-1}$ appears in the ladder but not the former. Furthermore,

$$c_{m,n}\binom{n-m}{k} = \begin{cases} c_{m,n-k}\binom{n}{k} & \text{if } k \neq n-m, \\ c_{m,n-k}\binom{n}{k} + c_{m,n} & \text{if } k = n-m. \end{cases}$$

It follows that $c_{m,m} = 0$ and, for $m < n$, $c_{m,n} = \frac{n!}{(n-m)!(m+1)!}c_{m,m+1}$. One can then readily check that we get the desired expression for L by setting $f_{m+1} = c_{m,m+1}/(m+1)!$. $\square$

Although we proved it for completeness, this result is well known; e.g. Panzer [Pan11] obtained an equivalent algebraic characterization. For the divided power coalgebra, the coproduct is defined by setting

$$\Delta(y^n) = \sum_{k=0}^{n} y^k \otimes y^{n-k}.$$

This also gives a Hopf algebra on $K[y]$, but the compatible algebra structure instead has the product $y^i \cdot y^j = \binom{i+j}{i}y^{i+j}$; nevertheless it is in fact isomorphic as a Hopf algebra to the binomial Hopf algebra via a scaling of coefficients. With that said, we will always work with the standard product on $K[y]$, meaning that in this case only the first statement of the universal property will apply; we will later see that interesting combinatorics arise regardless. A similar formula holds for Hochschild 1-cocycles in the divided power coalgebra with the integral replaced with a degree raising operator and the derivative with a degree lowering operator δ—its proof can be easily constructed by adapting the proof of Lemma 2.3 so we omit it.

Lemma 2.4. *A map L is a 1-cocycle operator for the divided power coalgebra on $K[y]$ if and only if*

$$L(y^n) = yF(\delta_y)y^n$$

for some power series $F(z) = \sum_{i \geqslant 0} f_i z^i$ in $K[[z]]$, where $\delta_y(y^n) = y^{n-1}$ if $n > 0$ and 0 otherwise.

We will write L_{bin} and L_{div} for 1-cocycles of the binomial and divided power coalgebras, respectively, with the underlying power series F implicitly carried along. Note that for both of these operators $\deg L(y^n) \leqslant n+1$ and, in particular, this bound is obtained if and only if $f_0 \neq 0$.

Over the next three sections, we will prove that

$$G(x, y) = xL_{bin}(\phi(G(x, y))) \tag{2.3}$$

and

$$G(x, y) = xL_{div}(\phi(G(x, y))) \tag{2.4}$$

are solved by certain weighted generating functions over connected weighted chord diagrams. At a high level, our proof strategy is as follows: a) expand the functional equations into recurrences which characterize the solution, b) apply induction to turn the recurrence into an equivalent generic combinatorial identity, then for each case, c) set up a map underlying the corresponding identity based on a decomposition of a weighted chord diagram into weighted subdiagrams, d) exhibit its inverse, proving that it is a bijection and therefore the identity holds, as required. We begin with steps (c) and (d) and the relevant chord diagram combinatorics.

3. Chord diagrams and their features

In this section we formally define chord diagrams and their features and properties that will be important in this context, as well as prove many basic facts about them.

Definition 3.1 (Chord diagram, intersection graph, crossing, nesting)**.** A *rooted chord diagram C of size n* is a perfect matching of $\{1, 2, \ldots, 2n\}$; the chord containing 1 is the *root* of C and we view the empty set $\varnothing$ as a diagram of size 0. By convention, the elements of C are ordered pairs (x, y) with $x < y$; x and y are called the *source* and *sink*, respectively, of chord (x, y). A subset $D \subseteq C$ is a *subdiagram* of C. The *directed intersection graph $G(C)$ of C* has the chords as vertices and two chords $c_1 = (x_1, y_1)$ and $c_2 = (x_2, y_2)$ with $x_1 < x_2$ joined by a directed edge $c_1 c_2$ if $x_2 < y_1 < y_2$. In this case, we say that c_2 is a *right neighbor of c_1* and c_1 is a *left neighbor of c_2*. Forgetting direction, the edge $c_1 c_2$ is also referred to as a *crossing* and c_1 and c_2 are said to *cross*. On the other hand, if $x_1 < x_2 < y_2 < y_1$ then c_2 is *nested under c_1* and together these two chords form a *nesting*.

Note that we treat a subdiagram D of C as a proper chord diagram on $\{1, 2, \ldots, 2|D|\}$ by applying an order-preserving bijection. In the sequel, any graph-theoretic notions used in the

Figure 3.1: Left: a linear representation of a decomposable chord diagram with two indecomposable components and three connected components. Right: a connected chord diagram C with three terminal chords with indices 4, 5, and 6 in the intersection order, which differs from the standard order on C.

context of a chord diagram or its elements should be understood as referring to the appropriate feature of its directed intersection graph (e.g. c_1 is in the neighborhood of c_2). We will also extend the notion of nesting to subdiagrams in the obvious way: $D' \subseteq C$ is nested under $D \subseteq C$ if each chord of D' is nested under every chord of D. Unsurprisingly, a diagram is called *nonnesting* (resp. *noncrossing*) if it contains no nestings (resp. crossings).

There are two representations of a chord diagram used in the literature. The circular representation involves arranging points labeled by $1, 2, \ldots, 2n$ on a circle and, for each chord, joining the source and sink points with a straight line. We can obtain the linear representation from the circular one by cutting the circle just before the root point labeled 1 and straightening the resulting curve, letting the lines corresponding to each chord bend into smooth curves lying above the straightened curve, and then deleting the curve (see Figure 3.1). While the circular representation becomes unrooted after dropping the labels, the linear representation is naturally rooted at the leftmost point and the element labels are determined by the linear order of the points. We will use the linear representation throughout this paper.

Definition 3.2 (Connectivity, connected diagram). The *vertex connectivity* $\kappa(C)$, or simply *connectivity*, of a diagram C is the vertex connectivity $\kappa(G(C))$ of its intersection graph, that is, the minimum number of vertices whose removal disconnects $G(C)$. The *edge connectivity* $\lambda(C)$ of C is defined similarly by removing edges instead of vertices. A diagram C is k-*connected* if $\kappa(C) \geqslant k$; in particular, it is *connected* if it is 1-connected.

A disconnected diagram can be equivalently defined as one which can be partitioned into two nonempty subdiagrams with no crossings between them. The strictly stronger notion of decomposability of a diagram arises by excluding both crossings and nestings between the two subdiagrams.

Definition 3.3 (Diagram concatenation, indecomposable diagram). Let C_1 and C_2 be diagrams. The *concatenation* of C_1 and C_2 is the diagram $C_1 C_2$ of size $|C_1| + |C_2|$ whose perfect matching restricts to C_1 on the first $2|C_1|$ elements and to C_2 on the next $2|C_2|$ elements (as subdiagrams). A diagram C is *decomposable* if it can be expressed as the concatenation of two smaller diagrams and *indecomposable* otherwise.

Figure 3.1 illustrates examples of a decomposable diagram and a connected diagram. Analogously to connected components, we refer to maximal nonempty indecomposable subdiagrams

as indecomposable components. Observe the following basic fact that we will use heavily for proofs involving induction.

Lemma 3.4. *The diagram obtained by removing the root chord of a connected diagram is indecomposable.*

3.1. 1-terminality

While the above definitions are largely standard in the combinatorics literature, the following are more unique to this context and most of them first appeared in a paper of Marie and Yeats [MY13] (see also [HY19, CY17, CYZ19, CY19]). Note that the directed intersection graph is acyclic, so it induces a partial order on the chords by reachability. We define several different total orders on the chords of a diagram C which extend this partial order.

Definition 3.5 (Standard order, intersection order). The *standard order* of C is given by the order of the sources of the chords of C. For connected C, the *intersection order* is defined recursively as follows: starting with 1, label the root chord of C with the next available label, then remove the root and label the resulting connected components recursively by the standard order of their roots.

The standard order will be used as the default order on a chord diagram unless stated otherwise. Note that the standard order and intersection order generally differ substantially (see Figure 3.1). If we replace 'connected' with 'indecomposable' and label the components by the reverse standard order of their roots then we get the *peeling order*, which for some purposes is in fact equivalent to the intersection order (see [CYZ19] for details). The weighted generating functions solving (2.3) and (2.4) will principally depend on the the positions or indices of certain special chords in the intersection order.

Definition 3.6 (Terminal chords and 1-terminal diagrams). Let C be a chord diagram. A chord $c \in C$ is *terminal* if it is incident to no outgoing edges in $G(C)$, that is, it has no right neighbors. These are the maximal elements in the reachability poset. A diagram C is *1-terminal* if the last chord is the only terminal chord.

Since the chord with rightmost sink in each connected component is necessarily terminal, it follows immediately from the definition that 1-terminal diagrams are connected. The indices of the terminal chords in a connected diagram will play an important role in both our generating function solutions and the rest of the paper. Accordingly, we will denote the index of the jth terminal chord in the intersection order of a diagram C by $t_j(C)$. We now record a series of basic facts about these orders and 1-terminal objects, most of which do not seem to have appeared in the existing literature. For the rest of this section let C be a connected diagram of size n with $t_1(C) = k$ and $c_1 < c_2 < \cdots < c_n$ be the chords of C in the intersection order. Note that if $t_1(C) = 1$, that is, the root chord is terminal, then it is the only chord of C, while if $t_1(C) = n$ then C is 1-terminal.

Lemma 3.7. *In the standard order, we also have $c_1 < c_2 < \cdots < c_k$; that is, the intersection order and standard order agree in a relative sense up to the first terminal chord, which is the chord with rightmost sink.*
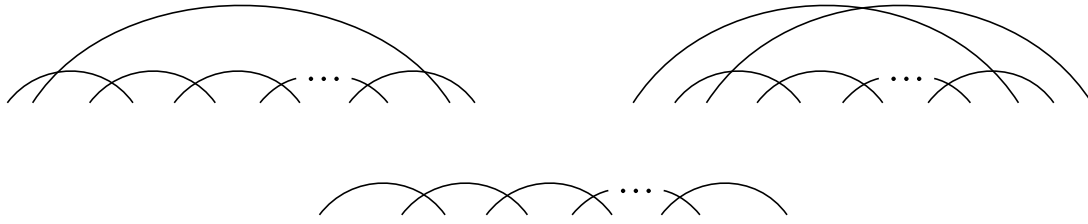
Figure 3.2: Top: top and bottom cycles, the only diagrams whose intersection graph form an induced cycle. Bottom: the unique diagram whose intersection graph forms a nonnesting induced path.

Proof. Note that the root chord comes first in the standard order and if we remove it to obtain an indecomposable diagram C', c_k is also the first terminal chord in the outermost connected component of C'. With these facts the result follows by applying induction to the outermost component. $\qquad\square$

The second part of this lemma was observed by Courtiel and Yeats [CY17] in their work on terminal chords. As a consequence, the intersection order and standard order are equivalent on 1-terminal diagrams. The other direction does not hold; there are diagrams with multiple terminal chords in which the two orders agree (e.g. take a root crossing a set of terminal chords which all pairwise nest).

Lemma 3.8. *The indecomposable components $C_1, C_2, \ldots, C_m$ remaining after removing $c_1, c_2, \ldots, c_k$ have no right neighbors in C.*

Proof. Since the intersection order extends the partial order on chords induced by the directed intersection graph, the chords $c_1, \ldots, c_k$ can only cross chords in $C_1 \cup \cdots \cup C_m$ on the left. Since these chords are the only neighbors of $C_1, \ldots, C_m$ by specification, the statement follows. $\qquad\square$

Note that there are exactly two diagrams whose undirected intersection graph is isomorphic to an induced cycle of size n; we call these the *top cycle* diagram and the *bottom cycle* diagram. This diagram representation (near-)uniqueness property was first observed by Bouchet [Bou94]. While no such property holds for induced paths, we gain representation uniqueness if we require that the path is also nonnesting (see Figure 3.2); this leads to the following observation.

Lemma 3.9. *There exists a nonnesting induced path in $\{c_1, c_2, \ldots, c_k\}$ from c_j to c_k for all $1 \leqslant j \leqslant k$. In particular, the chords $c_1, c_2, \ldots, c_k$ induce a 1-terminal subdiagram.*

Proof. If $n = 1$, the result holds trivially. Otherwise, remove the root and consider the outermost component D of the resulting indecomposable diagram. Inductively, for all $2 \leqslant j \leqslant k$ there is a nonnesting induced path $P_j \subseteq \{c_2, \ldots, c_k\}$ from c_j to c_k in D. Since C is connected, by the order extension property the source of c_2 lies before the sink of c_1. Furthermore, c_k either crosses the root or its source lies after the sink of the root. Thus some chord in P_2 crosses c_1; choose such a chord c_i with i maximum and let P_2' be the subpath of P_2 beginning at c_i. Then $\{c_1\} \cup P_2'$ is a nonnesting induced path from c_1 to c_k in C. $\qquad\square$
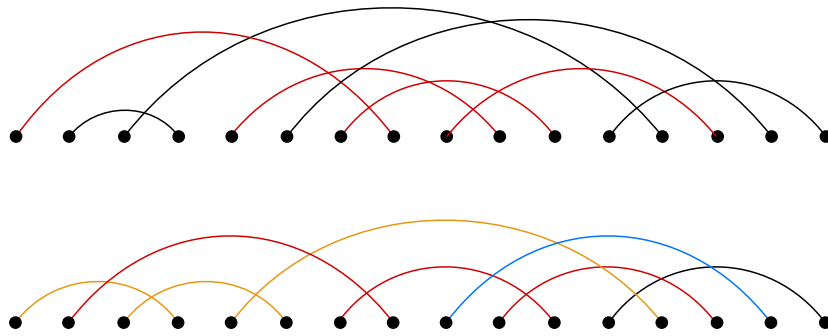
Figure 3.3: Above: a 1-terminal diagram with the traced subdiagram of the rightmost highlighted chord highlighted. Below: another 1-terminal diagram with the traced subdiagrams of the neighbors of the terminal chord colored. There is no nonnesting induced path between the third chord and fifth chord, in the standard order.

One can check that this proof actually implicitly constructs nonnesting induced paths to the first terminal chord defined by the property that the $(i + 1)$th chord of the path is the rightmost neighbor in $\{c_1, c_2, \ldots, c_k\}$ of the ith chord. It also gives a characterization of 1-terminality.

Corollary 3.10. *The following are equivalent.*

(i) C *is 1-terminal.*

(ii) $C - c_1$ *is 1-terminal.*

(iii) *There exists a nonnesting induced path from c to c_n for all $c \in C$.*

Proof. Lemma 3.9 gives the equivalence of (i) and (iii), while the fact that the root c_1 is not a right neighbor of any chord straightforwardly implies that (i) and (ii) are equivalent. □

The above results begin to illustrate how 1-terminality can be thought of as a more well-behaved notion of connectivity. In particular, for a vertex connectivity version of the above corollary, a version of (ii) no longer applies and we drop "nonnesting" to get a version of (iii). We will see further evidence for this view later in the paper. Figure 3.3 illustrates a 1-terminal diagram with two chords that are not linked by a nonnesting induced path, indicating that this result cannot be strengthened to get such a path between e.g. any two nonnesting chords absent a stronger hypothesis.

3.2. Grouping and tracing

The bijection we will construct in the next section involves decomposing a connected chord diagram into specific subdiagrams. This decomposition is constructed by first decomposing the 1-terminal part of the diagram revealed by Lemma 3.9 into certain 1-terminal subdiagrams, which we define presently. We begin with a key concept useful to defining these objects as well as additional aspects of decompositions and maps introduced later in the paper.
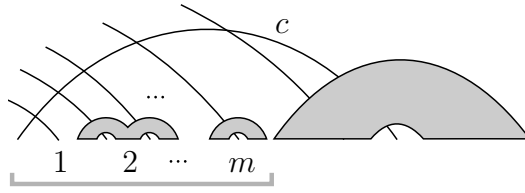
Figure 3.4: A representative visualization of the source-sink group, indicated by the grey bracket, of a chord c in a connected diagram of valency m.

Write $N_L(c)$ and $N_R(c)$ for the left and right neighbors, respectively, of a chord $c \in C$.

Definition 3.11 (Source-sink group). We say that a chord $c \in C$ is *attached* to an indecomposable subdiagram B of C if $\{c\}$ is not a connected component of $B \cup \{c\}$; symmetrically, B is also *attached* to c. Define the *source-sink group* of c to be the interval of endpoints containing:

- the source of c,

- the indecomposable components of $C - N_L(c)$ nested under c and not nested under any chord $c' > c$, and

- the sinks of $N_L(c)$ whose associated chord is either attached to one of the above indecomposable components or does not cross any chord $c' > c$.

The source-sink groups of C refers to the source-sink groups of the chords of C.

See Figure 3.4. More informally, we will also refer to chords as "attached" to their sources and sinks. Observe that that the source-sink group of c can also be characterized as the points between the source of c (inclusive) and the source of the next chord (exclusive) in the intersection order; while this characterization is simpler, it does not offer the local structural information of the above definition. Note that there may be no sinks in a source-sink group. Source-sink groups enable us to define a notion of *valency* for chords in a diagram. This is essentially a new structural interpretation of an iteratively-defined parameter called the covering number that featured in earlier work (see [HY19] and Section 8 for more details).

Definition 3.12. Define the *valency* of $c \in C$, written val(c), to be $k + \ell$ if there are exactly k left neighbors of c not attached to any chord $c' > c$ and after removing the left neighbors of c we are left with exactly ℓ indecomposable components immediately following the source of c.

Loosely speaking, in a local sense the valency is the number of connected pieces in the source-sink group of a chord. This notion of valency for a diagram should be thought of as playing the same role as outdegree for a tree, that is, the number of children of a vertex in a rooted tree. The chord in Figure 3.4 has valency m. As we will see, our decomposition preserves source-sink groups and therefore valencies. This will in particular gain importance in Section 5.

Let T be a 1-terminal diagram. By Lemma 3.8 the source-sink groups of T contain only a source and adjacent maximal interval of sinks. The source-sink group of a chord $c \in T$ contains no sinks precisely when c is the only chord of T or there is another source following the source of c.

Definition 3.13 (Traced subdiagram)**.** For $c \in T$, we construct the *traced subdiagram T_c of c* as follows. The chord c belongs to T_c. Beginning with $c' = c$, place in T_c every chord attached to a sink in the source-sink group of c', and then repeat this procedure with each newly added chord of T_c.

See Figure 3.3 for examples. Since for 1-terminal diagrams every chord attached to a sink in the source-sink group crosses the chord of the source to the left, traced subdiagrams are equivalently specified as follows: for any chord c' of $T - c$, c' is in T_c if and only if the last right neighbor of c' (in the standard order) is in T_c. In particular, we observe the following.

Lemma 3.14. *Traced subdiagrams T_c are 1-terminal and c is the terminal chord.*

The above observation together with the following result gives a unique decomposition of a 1-terminal diagram into smaller 1-terminal subdiagrams, after removing the terminal chord.

Lemma 3.15. *The traced subdiagrams of the neighbors of the terminal chord d of the 1-terminal diagram T partition $T - d$.*

Proof. If $|T| = 1$, the result trivially holds. Otherwise, the root chord c is either a neighbor of d or it is not. If it is, note that by 1-terminality there are no chords nested under the terminal chord. Then clearly $T_c = \{c\}$ and, since the last right neighbor of c is d, it is not contained in any other traced subdiagram besides T_d. Since traced subdiagrams are 1-terminal, by Corollary 3.10 it follows that all other traced subdiagrams (excluding T_d) are inherited from $T - c$. Then we get the required partition inductively or immediately if $T - c - d$ is empty. On the other hand, if c is not a neighbor of d then it is contained in the traced subdiagram of T of its rightmost neighbor, which exists since T is connected. Then, as before, inductively we get the required partition. $\square$

Although we will not need this fact, it is also worth observing that this implies that the traced subdiagram of the terminal chord of T is the entire diagram.

4. A recursive bijection

We are now ready to construct our decomposition of connected diagrams. The construction comes in the form of a map α sending each connected diagram C to a tuple of connected diagrams along with a partition of an interval $[j]$. The partition specifies how the connected diagrams are shuffled together to generate C.

As previously, let $c_1 < c_2 < \cdots < c_n$ be the chords of C in the intersection order and $j + 1$ be the index $t_1(C)$ of the first terminal chord of C.

Definition 4.1. We define the following.

- T: the 1-terminal diagram $\{c_1, \ldots, c_{j+1}\}$.

- $A_1, A_2, \ldots, A_k$: the indecomposable components of $C - \{c_1, \ldots, c_j\}$ nested under c_{j+1}. Neighbors of the terminal chord c_{j+1} may or may not be attached to such a component; for each that is not, we also include among these A_ℓ's an empty component and consider them attached to their paired neighbor chord. Note in particular that k is the valency of c_{j+1}.
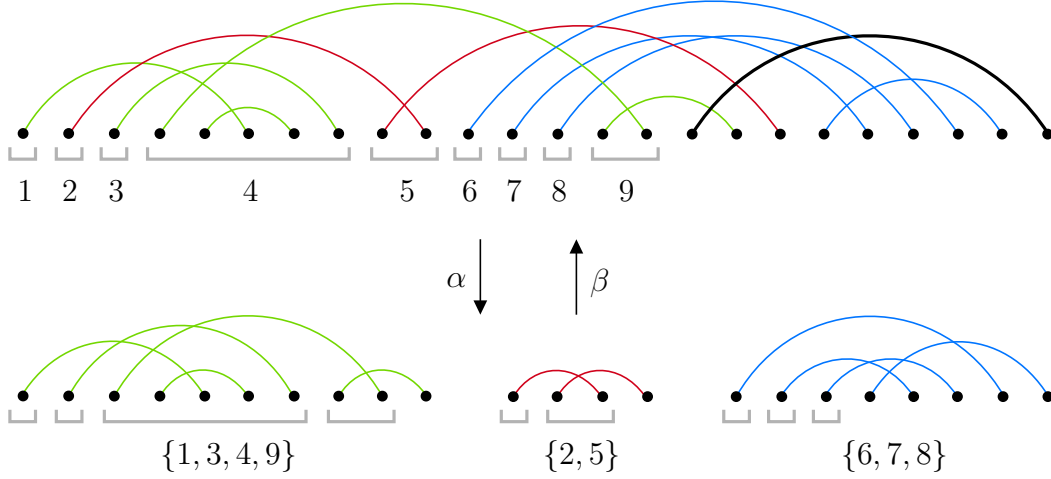
Figure 4.1: A connected diagram and its permuted decomposition defining the maps α and β. The source-sink groups used in the construction of β are indicated by the brackets below the three diagrams on the bottom of the figure and their derangement is then indicated below the diagram on the top of the figure.

- For all $1 \leqslant \ell \leqslant k$, D_ℓ: the union of the traced subdiagrams of T of each neighbor of c_{j+1} attached to component A_ℓ in C; if A_ℓ is empty this is simply the traced subdiagram of the neighbor defining A_ℓ above.

- For all $1 \leqslant \ell \leqslant k$, C_ℓ: the union of D_ℓ with all indecomposable components of $C - T$ attached to chords of D_ℓ in C.

- For all $1 \leqslant \ell \leqslant k$, I_ℓ: the subset $\{1 \leqslant i \leqslant j \mid c_i \in C_\ell\}$ of $[1, j]$ indicating which chords in $T - c_{j+1}$ belong to C_ℓ. Furthermore, set $i_\ell = |I_\ell|$.

- $\alpha(C) = ((C_1, I_1), (C_2, I_2), \ldots, (C_k, I_k))$.

Figure 4.1 illustrates an example of this construction for a representative diagram C. By Lemma 3.8 chords of T attach to indecomposable components of $C - T$ at sinks; in other words, the interval occupied by an indecomposable component of $C - T$ intersects at most one maximal interval of sinks of T. By the construction of traced subdiagrams, it follows that each indecomposable component of $C - T$ is attached to the chords of D_ℓ for at most one ℓ. Thus, we observe that $\{C_1, \ldots, C_k\}$ is a partition of $C - c_{j+1}$ by Lemma 3.15 and the fact that C is connected (since therefore every indecomposable component of $C - T$ is attached to a chord of $T - c_{j+1}$); note that this also implicitly uses the fact that every neighbor of c_{j+1} is in T since the intersection order is an extension of the reachability order. We also have the following properties.

Claim 4.2. *For all ℓ, (i) C_ℓ is connected and (ii) $t_1(C_\ell) \geqslant i_\ell$.*

Proof. Note that clearly each neighbor of c_{j+1} attached to A_ℓ has a path to every other attached neighbor since each cross a chord in the outermost connected component of A_ℓ by definition.

Furthermore, the traced subdiagram of T of a neighbor of c_{j+1} is connected since it is 1-terminal by Lemma 3.14. By construction, it follows that C_ℓ is connected since C is connected, giving (i). For (ii), note that either C_ℓ is constructed from the traced subdiagram of exactly one neighbor c_i of c_{j+1} or A_ℓ is nonempty. In the former case, c_i is the first terminal of C_ℓ, while in the latter case each chord of D_ℓ has a right neighbor in C_ℓ by the 1-terminality of traced subdiagrams. Thus, in either case, each neighbor of c_{j+1} in C_ℓ precedes (non-strictly) the first terminal chord of C_ℓ, which is necessarily either the neighbor c_i or in A_ℓ. Then another application of Lemma 3.14 yields the inequality $t_1(C_\ell) \geqslant i_\ell$. $\qquad\square$

We now show that α has an inverse, that is, define a map β such that $\beta \circ \alpha = \mathrm{id}$ and $\alpha \circ \beta = \mathrm{id}$. Suppose we are given a tuple $((C_1, I_1), \ldots, (C_k, I_k))$ with $C_1, \ldots, C_k$ connected diagrams and $\{I_1, \ldots, I_k\}$ a partition of $[1, j]$ with $1 \leqslant |I_\ell| \leqslant t_1(C_\ell)$ for all ℓ and $j = |I_1| + \cdots + |I_k|$.

Definition 4.3. We define the composed diagram C and map β as follows.

- For all $1 \leqslant \ell \leqslant k$, D_ℓ: the 1-terminal diagram induced by the first $|I_\ell|$ chords of C_ℓ in the intersection order.

- C': the diagram obtained by concatenating $C_1, \ldots, C_k$ and then arranging the source-sink groups corresponding to the first $|I_1|, \ldots, |I_k|$ chords (in the intersection order) of $C_1, \ldots, C_k$, respectively, in order according to the permutation induced by $I_1, \ldots, I_k$, maintaining the order of the points within each diagram C_ℓ.

- C: the diagram obtained from C' by adding a chord c with its sink in the rightmost position and source immediately following the source-sink groups corresponding to the first j chords of C' (in the intersection order).

- $\beta((C_1, I_1), \ldots, (C_k, I_k)) = C$.

A representative example of this construction is given in Figure 4.1.

Claim 4.4. *We have* $t_1(C) = j + 1$.

Proof. For all ℓ, clearly at least one source of C_ℓ lies to the left of the source of c while the rightmost sink of C_ℓ lies to the right of the source of c. Since C_ℓ is connected, it follows that c has a neighbor from each C_ℓ, implying that C is connected. Then by Lemma 3.7, c is the first terminal chord of C since its sink lies furthest to the right. Note that nonnesting paths of C_ℓ are preserved in C by the construction process; since the first terminal chord of C_ℓ clearly either crosses c or is nested under it, this implies that there is a nonnesting path from each of the first $|I_\ell|$ of C_ℓ to c, implying that $t_1(C) \geqslant |I_1| + \cdots + |I_\ell| + 1 = j + 1$ by Lemma 3.9. On the other hand, by the extension property of the intersection order, all the chords of $C_\ell - D_\ell$ come after the first terminal chord of C in the intersection order. Combined with the fact that only $|I_\ell|$ chords of D_ℓ have their sources to the left of the source of c, we see that $t_1(C) \leqslant j + 1$ by Lemma 3.7. We therefore infer that $t_1(C) = j + 1$, as required. $\qquad\square$

Claim 4.5. *The map β is the inverse of α.*

Proof. Observe that α partitions the points of a given connected diagram C lying before the source of the terminal chord c_{j+1} along source-sink groups. Then it follows that, for C in the domain of α and $((C_1, I_1), \ldots, (C_k, I_k))$ in the domain of β, we have $\beta(\alpha(C)) = C$ and $\alpha(\beta((C_1, I_1), \ldots, (C_k, I_k)))$ by construction and our prior conclusions about α and β. $\square$

The bijection α translates into the following result recursively enumerating connected diagrams by size and index of the first terminal chord.

Theorem 4.6. *Write $c_{n,j}$ for the number of connected diagrams of size n with $t_1(C) = j$. Then*

$$c_{n+1,j+1} = \sum_{k=1}^{n} \sum_{\substack{n_1 + \cdots + n_k = n \\ n_\ell \geqslant 1}} \sum_{\substack{i_1 + \cdots + i_k = j \\ 1 \leqslant i_\ell \leqslant n_\ell}} \binom{j}{i_1, \ldots, i_k} \sum_{j_1 \geqslant i_1} c_{n_1, j_1} \cdots \sum_{j_k \geqslant i_k} c_{n_k, j_k}.$$

This recurrence is implicit in the work of Marie and Yeats [MY13]. Later, an equivalent recurrence based on the root-share decomposition was obtained by Courtiel and Yeats [CY17]. While our decomposition is more complex, it also more clearly reveals the structure of connected diagrams and can be used to derive further information about certain additional diagram parameters, as shown in Section 5.

We now apply this decomposition to connected top-cycle-free diagrams. In this case the diagram ends up uniquely decomposing into a tuple of smaller top-cycle-free diagrams—the need to provide a shuffle-defining partition to accompany the decomposition effectively disappears. We specifically prove the following recurrence.

Theorem 4.7. *Write $t_{n,j}$ for the number of connected top-cycle-free diagrams of size n with $t_1(C) = j$. Then*

$$t_{n+1,j+1} = \sum_{k=1}^{n} \sum_{\substack{n_1 + \cdots + n_k = n \\ n_\ell \geqslant 1}} \sum_{\substack{i_1 + \cdots + i_k = j \\ 1 \leqslant i_\ell \leqslant n_\ell}} \sum_{j_1 \geqslant i_1} t_{n_1, j_1} \cdots \sum_{j_k \geqslant i_k} t_{n_k, j_k}.$$

Proof. Let C be a connected top-cycle-free diagram of size $n + 1$ with $t_1(C) = j + 1$ and $c_1 < c_2 < \cdots < c_{n+1}$ the chords of C in the intersection order. As previously, let $\alpha(C) = ((C_1, I_1), \ldots, (C_k, I_k))$; Figure 4.2 displays a representative example. Note that $C_1, \ldots, C_k$ are clearly top-cycle-free since they are subdiagrams of the top-cycle-free diagram C.

Claim 4.8. *$I_1, \ldots, I_k$ are intervals.*

Proof. Suppose to the contrary that I_ℓ is not an interval for some ℓ. Then there exists a block $I_{\ell'}$ such that I_ℓ and $I_{\ell'}$ either nest or cross, that is, there are $r, s \in I_\ell$ and $t \in I_{\ell'}$ such that $r < t < s$. By construction, each subdiagram D_ℓ of C_ℓ contains a neighbor of the first terminal chord c_{j+1} of C and each such neighbor lies before the first terminal chord of C_ℓ in the intersection order. Since D_ℓ is connected, there exists a path P in D_ℓ from c_r to c_s. By construction of $D_{\ell'}$ and Lemma 3.9, there exists a nonnesting path Q in $D_{\ell'}$ from c_t to a neighbor of c_{j+1} in $D_{\ell'}$; let $Q' = Q \cup \{c_{j+1}\}$. Since $r < t < s$, by Lemma 3.7 $c_r < c_t < c_s$ in the standard order,
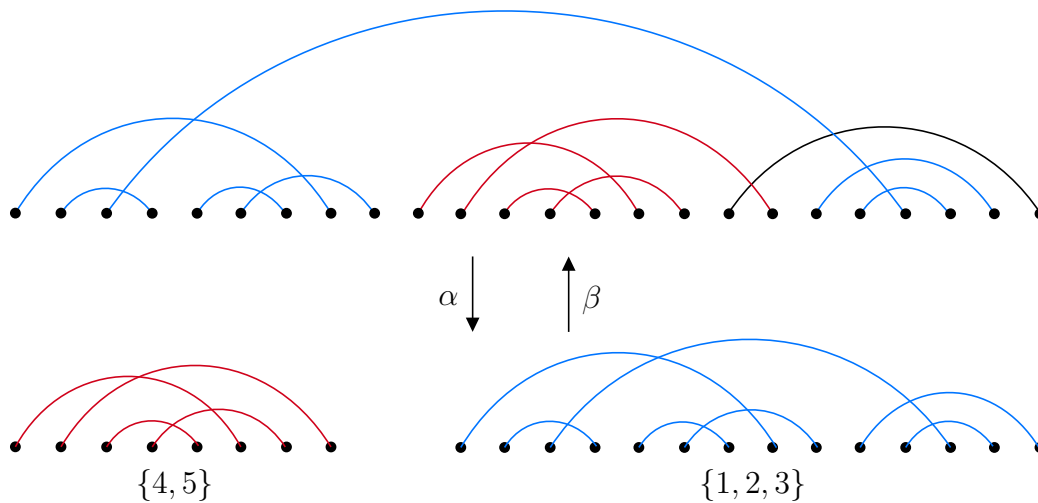
Figure 4.2: A top-cycle-free diagram and its decomposition defining the maps α and β.

implying that P and Q cross, that is, there is a chord c in P and a chord c' in Q such that c and c' cross. Let P' be a nonnesting path in D_ℓ from c to a neighbor of c_{j+1} in D_ℓ, which again exists by construction and Lemma 3.9. Then $P' \cup Q'$ contains two internally-disjoint nonnesting paths of length at least three with the same first and last chords (in the standard order), so one can easily see that it contains a top cycle as a subdiagram. But then C is not top-cycle-free, a contradiction. $\qquad\square$

Now fix a tuple $((C_1, I_1), \ldots, (C_k, I_k))$ with $C_1, \ldots, C_k$ connected top-cycle-free diagrams and $\{I_1, \ldots, I_k\}$ a partition of $[1, j]$ into intervals with $1 \leqslant |I_\ell| \leqslant t_1(C_\ell)$ for all ℓ and $j = |I_1| + \cdots + |I_k|$, and write $C = \beta((C_1, I_1), \ldots, (C_k, I_k))$ and let c be the first terminal chord of C. Suppose C contains a top cycle subdiagram A. Clearly $C - c$ is top-cycle-free since its connected components are exactly $C_1, \ldots, C_k$. Then it follows that A must contain c and, since cycles are 2-connected, be a subdiagram of $C_\ell \cup \{c\}$ for some ℓ. Write $A = \{c'_1, \ldots, c'_m, c\}$, where $c'_1 < c'_2 < \cdots < c'_m < c$ in the standard order. Without loss of generality we may assume that A is chosen with c'_2 maximum (in the standard order). Then, since C_ℓ is top-cycle-free, there is no path nested under c'_2 from a chord of $A' = A - \{c'_1, c'_2, c\}$ to a right neighbor of t_2, implying that A' is a subset of the source-sink group of c'_2. By construction it follows that c'_m cannot cross c, a contradiction. So C is top-cycle-free.

Since α is a bijection and there is exactly one partition of $[1, j]$ into a fixed number of intervals with specified ordered sizes, this completes the proof. $\qquad\square$

5. Solving tree-like equations

We are now ready to solve tree-like equations (2.3) and (2.4). The solutions come in the form of weighted generating functions for certain chord diagram classes.

Given a connected diagram C and a sequence of weights $(\phi_k)_{k \geqslant 0}$ in a field K, we associate a weight ϕ_k with each chord $c \in C$ of valency k (recall Definition 3.12 of Section 3.2). Then

we define the *weight* of C to be

$$\phi_C = \prod_{c \in C} \phi_{\text{val}(c)}.$$

This is exactly the same way weights of trees are traditionally defined, at least in the context of tree models and hook lengths [FS09, KP13].

Theorem 5.1. *The functional equation*

$$G(x, y) = xL(\phi(G(x, y))), \tag{5.1}$$

with $\phi(z) = \sum_{k \geqslant 0} \phi_k z^k$ for $\phi_k \in K$, is uniquely solved by

$$G(x, y) = \sum_{C \in \mathcal{C}} f_C \phi_C x^{|C|} \frac{L_{bin}(y^{t_1(C)-1})}{(t_1(C) - 1)!} \quad \text{if} \quad L = L_{bin} \tag{5.2}$$

and

$$G(x, y) = \sum_{C \in \mathcal{C}_{top}} f_C \phi_C x^{|C|} L_{div}(y^{t_1(C)-1}) \quad \text{if} \quad L = L_{div}, \tag{5.3}$$

where $\mathcal{C}$ is the set of connected chord diagrams, $\mathcal{C}_{top}$ is the set of connected top-cycle-free chord diagrams, that is, connected diagrams with no top cycle subdiagram, $\phi_C = \prod_{c \in C} \phi_{\text{val}(c)}$, and

$$f_C = f_0^{|C|-k} f_{t_2(C)-t_1(C)} f_{t_3(C)-t_2(C)} \cdots f_{t_k(C)-t_{k-1}(C)}$$

for a connected diagram C with k terminal chords and f_i the coefficients of the power series F specifying L.

In other words, when L is a polynomial 1-cocycle operator Equation (5.1) is solved by a generating function for a certain family of connected weighted chord diagrams where each term is weighted by a monomial in the coefficients defining L determined by the size of the diagram, the number of terminal chords, and the differences between the indices of consecutive terminal chords in the intersection order. The diagrams are counted by their size in the x variable and one less than the index of the first terminal chord in the y variable. While (5.3) can be thought of as ordinary in both variables, (5.2) should be viewed as ordinary in x and exponential in y, although the fact that $L(y^{t_1(C)-1})$ appears in the series rather $y^{t_1(C)-1}$ makes this less than strictly true. One could account for this by instead regarding both series as ordinary generating functions for a set of polynomials $\{p_C(y)\}$ indexed by a class of weighted chord diagrams. It is notable that the monomial f_C is determined by the gaps between terminal chord indices, not the indices themselves, indicating that it is their relative position that matters, not their absolute position.

Recall our strategy for proving Theorem 5.1 is as follows: 1) show that the decomposition defined in Section 4 yields suitable weighted versions of the combinatorial identities in Theorems 4.6 and 4.7, 2) apply induction to turn these identities into equivalent recurrences for the coefficients in the x variable, and 3) demonstrate that these recurrences are simply an expansion of the corresponding tree-like equations.

We begin with step 1. For this we will need certain statements about how the parameters f_C and ϕ_C behave under the bijection α. Let C be a connected diagram of size n with $t_1(C) = j+1$, T be its 1-terminal part, and $((C_1, I_1), \ldots, (C_k, I_k))$ be the image of C under α. Carry over all other notation from Section 4 and specifically Definition 4.1.

Lemma 5.2. *We have*

$$\phi_C = \phi_k \phi_{C_1} \cdots \phi_{C_k}.$$

Proof. Clearly the valency of the terminal chord c_{j+1} is k. Furthermore, for each chord $c \in C_\ell$ the valency of c in C and C_ℓ is equal by construction. Then the identity follows. $\square$

Now let $B_1, \ldots, B_m$ be the components of $C - T$ listed in the intersection order of C; that is, all chords of B_1 come before all chords of B_2, and so on. We require a lemma which says that f_C is determined by $f_D, f_{B_1}, \ldots, f_{B_m}$ and the index of the first terminal chords of $B_1, \ldots, B_m$ in the intersection order of C.

Lemma 5.3. *We have*

$$f_C = f_D f_{t_1(B_1)} f_{B_1} \cdots f_{t_1(B_m)} f_{B_m}.$$

In other words, $f_C = f_{C-B_m} f_{t_1(B_m)} f_{B_m}$.

Proof. By Lemma 3.8, terminal chords of B_i are terminal in C and vice versa for all i. Furthermore, by Lemma 3.9 T is 1-terminal both as a diagram and as a subdiagram of C. Thus every terminal chord of C corresponds bijectively to a terminal chord in $T, B_1, \ldots, B_k$. Furthermore, clearly the intersection orders on $T, B_1, \ldots, B_k$ agree with the intersection order on C (in the sense that $c \prec c'$ in T or B_i if and only if $c \prec c'$ in C for $c, c' \in T$ or $c, c' \in B_i$ for some i) by construction. It follows that the number of terminal chords of C is equal to the sum of the number of terminal chords in T and $B_1, \ldots, B_k$. We also further infer by construction that every difference $t_{i+1}(C) - t_i(C)$ corresponds uniquely to either a difference of consecutive terminal chord indices in some B_i or the difference between the index in C of the last terminal chord of B_{i-1} and the index in C of the first terminal chord of B_i, that is, $t_1(B_i)$. The desired equality follows from these two observations. $\square$

This gives the required equality.

Lemma 5.4. *We have*

$$f_C = f_{t_1(C_1)-i_1} f_{C_1} \cdots f_{t_1(C_k)-i_k} f_{C_k}.$$

Proof. By Lemma 5.3 applied to f_C and $f_{C_1}, \ldots, f_{C_n}$, we may assume that $C - T - \bigcup_\ell A_\ell$ is empty, since the corresponding terms in the monomials can simply be cancelled from both sides. Then $C_\ell = D_\ell \cup A_\ell$. By our observations in the proof of the claim above, the chords of D_ℓ are the first i_ℓ chords of C_ℓ in the intersection order. This implies that

$$f_{C_\ell} = f_{D_\ell \cup A_\ell} = \begin{cases} f_0^{i_\ell} A_\ell & \text{if } A_\ell \text{ nonempty,} \\ f_0^{i_\ell - 1} & \text{otherwise,} \end{cases}$$

$t_1(A_\ell) = t_1(C_\ell) - i_\ell$ (which is zero if and only if A_ℓ is empty), and

$$f_T = f_0^j = f_0^{i_1 + \cdots + i_k} = f_0^{i_1} \cdots f_0^{i_k}.$$

Then by Lemma 5.3

$$
\begin{aligned}
f_C &= f_T f_{t_1(A_1)} f_{A_1} \cdots f_{t_1(A_k)} f_{A_k} \\
&= f_0^{i_1} \cdots f_0^{i_k} f_{t_1(C_1)-i_1} f_{A_1} \cdots f_{t_1(C_k)-i_k} f_{A_k} \\
&= f_{t_1(C_1)-i_1} f_{C_1} \cdots f_{t_1(C_k)-i_k} f_{C_k}. \qquad \square
\end{aligned}
$$

With this we can give the proof.

Proof of Theorem 5.1. Combining the bijection α, the proofs of Theorems 4.6 and 4.7, and Lemmas 5.2 and 5.4 we obtain the following identities:

$$
\sum_{\substack{C \in \mathcal{C} \\ |C|=n+1 \\ t_1(C)=j+1}} f_C \phi_C = \sum_{k=1}^{n} \phi_k \sum_{\substack{n_1+\cdots+n_k=n \\ n_\ell \geqslant 1}} \sum_{\substack{i_1+\cdots+i_k=j \\ 1 \leqslant i_\ell \leqslant n_\ell}} \binom{j}{i_1, \ldots, i_k} \tag{5.4}
$$

$$
\times \left(\sum_{\substack{C_1 \in \mathcal{C} \\ |C_1|=n_1 \\ t_1(C_1) \geqslant i_1}} f_{t_1(C_1)-i_1} f_{C_1} \phi_{C_1} \right) \cdots \left(\sum_{\substack{C_k \in \mathcal{C} \\ |C_k|=n_k \\ t_1(C_k) \geqslant i_k}} f_{t_1(C_k)-i_k} f_{C_k} \phi_{C_k} \right)
$$

and

$$
\sum_{\substack{C \in \mathcal{C}(T_{\geqslant 3}) \\ |C|=n+1 \\ t_1(C)=j+1}} f_C \phi_C = \sum_{k=0}^{n} \phi_k \sum_{\substack{n_1+\cdots+n_k=n \\ n_\ell \geqslant 1}} \sum_{\substack{i_1+\cdots+i_k=j \\ 1 \leqslant i_\ell \leqslant n_\ell}}
$$

$$
\times \left(\sum_{\substack{C_1 \in \mathcal{C}(T_{\geqslant 3}) \\ |C_1|=n_1 \\ t_1(C_1) \geqslant i_1}} f_{t_1(C_1)-i_1} f_{C_1} \phi_{C_1} \right) \cdots \left(\sum_{\substack{C_k \in \mathcal{C}(T_{\geqslant 3}) \\ |C_k|=n_k \\ t_1(C_k) \geqslant i_k}} f_{t_1(C_k)-i_k} f_{C_k} \phi_{C_k} \right).
$$

We require a slightly different but equivalent form of these identities with an extra term added via an additional outermost series on both sides. This essentially matches the left hand side to

the innermost series on the right hand side. In particular we instead work with

$$\sum_{j=i-1}^{n} f_{j+1-i} \sum_{\substack{C \in \mathcal{C} \\ |C|=n+1 \\ t_1(C)=j+1}} f_C \phi_C - f_0 \mathbb{1}_{n=0}$$

$$= \sum_{j=\max\{i-1,1\}}^{n} f_{j+1-i} \sum_{k=1}^{n} \phi_k \sum_{\substack{n_1+\cdots+n_k=n \\ n_\ell \geqslant 1}} \sum_{\substack{i_1+\cdots+i_k=j \\ 1\leqslant i_\ell \leqslant n_\ell}} \binom{j}{i_1,\ldots,i_k}$$

$$\times \left(\sum_{\substack{C_1 \in \mathcal{C} \\ |C_1|=n_1 \\ t_1(C_1)\geqslant i_1}} f_{t_1(C_1)-i_1} f_{C_1} \phi_{C_1} \right) \cdots \left(\sum_{\substack{C_k \in \mathcal{C} \\ |C_k|=n_k \\ t_1(C_k)\geqslant i_k}} f_{t_1(C_k)-i_k} f_{C_k} \phi_{C_k} \right)$$

and

$$\sum_{j=i-1}^{n} f_{j+1-i} \sum_{\substack{C \in \mathcal{C}(T_{\geqslant 3}) \\ |C|=n+1 \\ t_1(C)=j+1}} f_C \phi_C - f_0 \mathbb{1}_{n=0}$$

$$= \sum_{j=\max\{i-1,1\}}^{n} f_{j+1-i} \sum_{k=1}^{n} \phi_k \sum_{\substack{n_1+\cdots+n_k=n \\ n_\ell \geqslant 1}} \sum_{\substack{i_1+\cdots+i_k=j \\ 1\leqslant i_\ell \leqslant n_\ell}}$$

$$\times \left(\sum_{\substack{C_1 \in \mathcal{C}(T_{\geqslant 3}) \\ |C_1|=n_1 \\ t_1(C_1)\geqslant i_1}} f_{t_1(C_1)-i_1} f_{C_1} \phi_{C_1} \right) \cdots \left(\sum_{\substack{C_k \in \mathcal{C}(T_{\geqslant 3}) \\ |C_k|=n_k \\ t_1(C_k)\geqslant i_k}} f_{t_1(C_k)-i_k} f_{C_k} \phi_{C_k} \right),$$

where $\mathbb{1}_{n=0} = 1$ if $n = 0$ and 0 otherwise. One can easily check that these are equivalent equalities. Now we translate these identities into polynomial recurrences. Note first that applying L_{bin} to the standard basis of $K[y]$ gives

$$L_{bin}(y^n) = \int_0^y F\left(\frac{d}{dt}\right) t^n dt = \int_0^y \sum_{i \geqslant 0} f_i \frac{d^i}{dt^i} t^n dt$$

$$= \int_0^y \sum_{i=0}^{n} f_i \frac{n!}{(n-i)!} t^{n-i} dt$$

$$= n! \sum_{i=1}^{n+1} f_{n+1-i} \frac{y^i}{i!}, \tag{5.5}$$

while applying L_{div} similarly gives

$$L_{div}(y^n) = yF(d_y)y^n = \sum_{i=1}^{n+1} f_{n+1-i} y^i. \tag{5.6}$$

Focusing on the binomial 1-cocycle case, define

$$h_n(y) = \sum_{C \in \mathcal{C}_n} f_C \phi_C \frac{L_{bin}(y^{t_1(C)-1})}{(t_1(C)-1)!}.$$

We aim to show that

$$h_{n+1}(y) = L_{bin}(1)\mathbb{1}_{n=0} + \sum_{k=1}^{n} \sum_{\substack{n_1+\cdots+n_k=n \\ n_\ell \geqslant 1}} \phi_k L_{bin}(h_{n_1}(y) \cdots h_{n_k}(y)). \tag{5.7}$$

Applying Equation (5.5) to the definition of $h_n(y)$ yields

$$h_n(y) = \sum_{C \in \mathcal{C}_n} f_C \phi_C \sum_{i=1}^{t_1(C)} f_{t_1(C)-i} \frac{y^i}{i!} = \sum_{i=1}^{n} \left(\sum_{\substack{C \in \mathcal{C} \\ |C|=n \\ t_1(C) \geqslant i}} f_{t_1(C)-i} f_C \phi_C \right) \frac{y^i}{i!},$$

thereby expressing $h_n(y)$ in standard polynomial form. Then

$$\phi_k L_{bin}(h_{n_1}(y) \cdots h_{n_k}(y))$$

$$= \phi_k L_{bin}\left(\sum_{i_1=0}^{n_1} \left(\sum_{\substack{C_1 \in \mathcal{C} \\ |C_1|=n_1 \\ t_1(C_1) \geqslant i_1}} f_{t_1(C_1)-i_1} f_{C_1} \phi_{C_1} \right) \frac{y^{i_1}}{i_1!} \cdots \sum_{i_k=0}^{n_k} \left(\sum_{\substack{C_k \in \mathcal{C} \\ |C_k|=n_k \\ t_1(C_k) \geqslant i_k}} f_{t_1(C_k)-i_k} f_{C_k} \phi_{C_k} \right) \frac{y^{i_k}}{i_k!} \right)$$

$$= \phi_k \sum_{m=0}^{n} L_{bin}(y^m) \sum_{\substack{i_1+\cdots+i_k=m \\ 0 \leqslant i_\ell \leqslant n_\ell}} \frac{1}{i_1! \cdots i_k!}$$

$$\times \left(\sum_{\substack{C_1 \in \mathcal{C} \\ |C_1|=n_1 \\ t_1(C_1) \geqslant i_1}} f_{t_1(C_1)-i_1} f_{C_1} \phi_{C_1} \right) \cdots \left(\sum_{\substack{C_k \in \mathcal{C} \\ |C_k|=n_k \\ t_1(C_k) \geqslant i_k}} f_{t_1(C_k)-i_k} f_{C_k} \phi_{C_k} \right)$$

$$= \phi_k \sum_{m=0}^{n} \sum_{i=0}^{m+1} f_{m+1-i} \frac{y^i}{i!} \sum_{\substack{i_1+\cdots+i_k=m \\ 0 \leqslant i_\ell \leqslant n_\ell}} \frac{m!}{i_1! \cdots i_k!}$$

$$\times \left(\sum_{\substack{C_1 \in \mathcal{C} \\ |C_1|=n_1 \\ t_1(C_1) \geqslant i_1}} f_{t_1(C_1)-i_1} f_{C_1} \phi_{C_1} \right) \cdots \left(\sum_{\substack{C_k \in \mathcal{C} \\ |C_k|=n_k \\ t_1(C_k) \geqslant i_k}} f_{t_1(C_k)-i_k} f_{C_k} \phi_{C_k} \right)$$

$$= \sum_{i=0}^{n+1} \frac{y^i}{i!} \sum_{m=\max\{i-1,0\}}^{n} f_{m+1-i} \phi_k \sum_{\substack{i_1+\cdots+i_k=m \\ 0 \leqslant i_\ell \leqslant n_\ell}} \binom{m}{i_1, \ldots, i_k}$$

$$\times \left(\sum_{\substack{C_1 \in \mathcal{C} \\ |C_1|=n_1 \\ t_1(C_1) \geqslant i_1}} f_{t_1(C_1)-i_1} f_{C_1} \phi_{C_1} \right) \cdots \left(\sum_{\substack{C_k \in \mathcal{C} \\ |C_k|=n_k \\ t_1(C_k) \geqslant i_k}} f_{t_1(C_k)-i_k} f_{C_k} \phi_{C_k} \right),$$

where the second equality follows from the linearity of L. Consequently, Equation (5.7) follows by applying our earlier combinatorial identity and rearranging and reindexing appropriately. We can perform nearly identical calculations to derive the recurrence

$$h_{n+1}(y) = L_{div}(1)\mathbb{1}_{n=0} + \sum_{k=1}^{n} \sum_{\substack{n_1+\cdots+n_k=n \\ n_\ell \geqslant 1}} \phi_k L_{div}(h_{n_1}(y)\cdots h_{n_k}(y))$$

for polynomials $h_n(y) = \sum_{C\in\mathcal{C}_n(T_{\geqslant 3})} f_C \phi_C L_{div}(y^{t_1(C)-1})$. It remains only to observe that writing $G(x,y) = \sum_{i\geqslant 1} h_i(y)x^i$ implies that

$$G(x,y) = xL(1) + x\sum_{k\geqslant 1}\sum_{n\geqslant 1}\sum_{\substack{n_1+\cdots+n_k=n \\ n_\ell \geqslant 1}} \phi_k L(h_{n_1}(y)\cdots h_{n_k}(y))x^n$$

$$= x\phi_0 L(1) + xL\left(\sum_{k\geqslant 1}\sum_{n\geqslant 1}\sum_{\substack{n_1+\cdots+n_k=n \\ n_\ell \geqslant 1}} \phi_k h_{n_1}(y)\cdots h_{n_k}(y)x^n\right)$$

$$= xL\left(\sum_{k\geqslant 0}\phi_k\left(\sum_{i\geqslant 1} h_i(y)x^i\right)^k\right)$$

$$= xL(\phi(G(x,y)))$$

for L either of the binomial or divided power 1-cocycle, proving that the polynomial recurrences are equivalent to the corresponding tree-like equations. $\qquad\square$

6. Connections to other combinatorial objects

We now turn to considering various bijective combinatorics arising from the decompositions and generating functions obtained in prior sections. While Theorem 4.7 in principle provides sufficient information to obtain an explicit formula for the counting sequence of $\mathcal{C}(T_{\geqslant 3})$, the nested composition-indexed series contained in the recurrence makes this a difficult task in practice. For this we turn to instead applying a bijective approach, for which our decomposition will prove helpful. Along the way we explore several connections between top-cycle-free diagrams and other natural combinatorial objects.

In this context, a *triangulation* T is a plane graph in which every bounded face is a triangle; for technical reasons we also require that a single edge counts as a triangulation. Triangulation T is *rooted* if it has a distinguished edge, the *root*, incident to the outer face; we will only work with rooted triangulations. As is standard in the literature, we consider such triangulations up to root-preserving isomorphism. *Exterior vertices* of T are incident to its boundary face, while all other vertices of T are *interior vertices*.

Theorem 6.1. *There is a bijection ω between connected top-cycle-free diagrams with n chords and i the index of the first terminal chord and triangulations with $n-i$ interior vertices and $i+1$ exterior vertices.*

In 1964, William G. Brown [Bro64] explicitly enumerated (rooted) triangulations with n interior vertices and $m + 3$ exterior vertices by deriving and solving a functional equation for the associated bivariate ordinary generating function, showing their number to be

$$\frac{2(2m+3)!(4n+2m+1)!}{m!(m+2)!n!(3n+2m+3)!}.$$

From Theorems 6.1 it follows that we get an explicit count for the corresponding top-cycle-free diagrams..

Corollary 6.2. *The number of connected top-cycle-free diagrams with n chords and $t_1 = i$ is*

$$\frac{2(2i-1)!(4n-2i-3)!}{(i-2)!i!(n-i)!(3n-i-1)!} = \frac{i-1}{(4n-2i-1)(2n-i-1)}\binom{2i-1}{i}\binom{4n-2i-1}{n-i}.$$

6.1. Bridgeless maps

We solved the tree-like equation

$$G(x, y) = xL(\phi(G(x, y))) \tag{6.1}$$

with weighted generating functions for certain classes of connected chord diagrams. What other combinatorial objects index these generating functions? Originally, in [MY13], Marie and Yeats solved the unweighted version of (6.1) with $L = L_{bin}$ by passing from chord diagrams to rooted plane binary trees. This essentially amounts to showing that there is a recursively-defined bijection, based on the root-share decomposition, between rooted connected chord diagrams and rooted plane binary trees with two recursively-defined properties. These properties are somewhat technical and based on a labeling of the leaves induced via the bijection by the intersection order on the chords of the associated diagram.

Later, Courtiel, Yeats, and Zeilberger [CYZ19] discovered a much nicer type of object, combinatorial maps, that could substitute for connected chord diagrams. A *(rooted) combinatorial map* is a transitive permutation representation of the group $\langle \sigma, \alpha \mid \alpha^2 = 1 \rangle$ with a distinguished fixed point for the action of α (the root). It can be represented by a connected graph of half edges, each paired with at most one other half-edge to form an edge, with a cyclic order of the half-edges incident to each vertex and the root a vertex attached to a distinguished "dangling" half-edge. Such a map inherits certain properties of this underlying graph; in particular, it is *bridgeless* if its graph is bridgeless, that is, 2-edge-connected. Other properties require a map-specific definition: it is *planar* if its Euler characteristic is 2 (see e.g. [CYZ19] for the definition of the Euler characteristic).

Theorem 6.3 (Courtiel, Yeats, and Zeilberger [CYZ19])**.** *There exists a bijection θ between connected diagrams and bridgeless maps such that*

- *chords correspond to edges;*

- *terminal chords correspond to vertices;*

- *the position t_1 of the first terminal chord corresponds to the indegree $\deg^-_{DFS,1}$ of the root vertex v_1 under the orientation induced by the rightmost depth-first search.*

For brevity, we omit the definition of the rightmost depth-first search and associated orientation referenced in this theorem; see Section 5.5 of [CYZ19] for these details. This bijection θ also transfers the parameters involved in defining the weights f_C and ϕ_C, namely, the differences $t_j - t_{j-1}$ between the indices of the jth and $(j-1)$th terminal chords in the intersection order as well as chord valencies, into corresponding parameters on the associated bridgeless map.

It turns out top-cycle-free diagrams also independently arose in the work of Courtiel, Yeats, and Zeilberger as the image of the bijection θ on a natural subset of bridgeless maps: those which are planar.

Theorem 6.4 (Courtiel, Yeats, and Zeilberger [CYZ19])**.** *Under θ, planar bridgeless maps are in bijection with connected top-cycle-free diagrams.*

Furthermore, changing "connected" to "indecomposable" corresponds to dropping "bridgeless" for both this result and Theorem 6.3. It follows from the work of Courtiel, Yeats, and Zeilberger that just as there is a bridgeless map view of (5.2), there is also a planar bridgeless map view of (5.3).

It was first proved by Tutte [Tut62] that there are

$$\frac{2}{n(n+1)}\binom{4n+1}{n-1} \tag{6.2}$$

triangulations with n internal vertices and 3 external vertices, while Wash and Lehman [WL75] proved that this also counts the number of rooted planar bridgeless maps with n edges. Bijections connecting these two sets of objects were later given by Wormald [Wor80], Fusy [Fus10], and Fang [Fan18], with the former two obtained recursively and the latter directly. Theorems 6.4 and 6.1 combine to yield a finer explicit count for planar bridgeless maps, refined by the indegree parameter defined above.

Corollary 6.5. *The number of planar bridgeless maps with n edges and $\deg^-_{DFS,1} = i$ is*

$$\frac{i-1}{(4n-2i-1)(2n-i-1)}\binom{2i-1}{i}\binom{4n-2i-1}{n-i}.$$

6.2. Proof of Theorem 6.1

We will use the unique decomposition described in Section 4 to recursively define our bijection. There is exactly one (connected top-cycle-free) diagram of size 1, namely, a single chord, and we map it to the unique (rooted) triangulation with no interior vertices and 2 exterior vertices: a single edge. So, explicitly, ω maps a single chord to a single edge. Now fix a connected top-cycle-free diagram C of size $n \geqslant 2$. Applying the unique decomposition from previous sections, we get connected top-cycle-free subdiagrams $C_1, \ldots, C_k$ and integers $i_1, \ldots, i_k$ with $i_1 + \cdots + i_k = t_1(C) - 1$ and $1 \leqslant i_\ell \leqslant t_1(C_\ell)$ for all $1 \leqslant \ell \leqslant k$; we have skipped the intervals $I_1, \ldots, I_k$ because their lengths $i_1, \ldots, i_k$ are sufficient to specify the decomposition and define the bijection ω. Then inductively we obtain image triangulations $T_1, \ldots, T_k$ of $C_1, \ldots, C_k$ under ω; write $t_\ell = t_1(C_\ell)$ and $v_{\ell,0}, \ldots, v_{\ell,t_\ell}$ for the exterior vertices of T_ℓ read counterclockwise
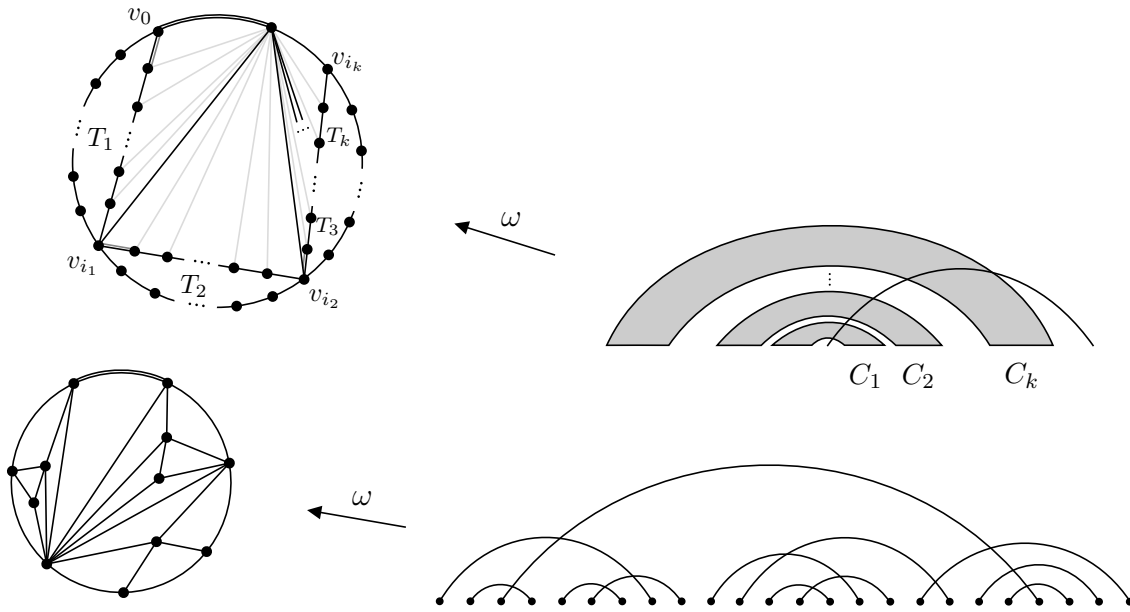
Figure 6.1: Above: the recursive construction of a triangulation and its image chord diagram under the bijection ω. The exterior vertex labels are taken from the decomposition map γ. Below: an example of the bijection applied to the connected top-cycle-free diagram from Figure 4.2.

starting at the leftmost vertex $v_{\ell,0}$ of the root edge (so, in particular, $v_{\ell,0}v_{\ell,t_\ell}$ is the root edge). Then we construct triangulation T as follows:

1. Join $T_1, \ldots, T_k$ in that order by identifying $v_{\ell-1,i_\ell}$ and $v_{\ell,0}$.

2. Add a new vertex v and connect it with an edge to $v_{1,0}$ and v_{k,i_k}; this creates a single new bounded face.

3. Root the graph at edge $v_{1,0}v$.

4. While keeping the graph simple, add an edge from v to every vertex incident to the newly created bounded face.

See Figure 6.1 for a visual representation of the construction as well as an explicit example. We then set $\omega(C) = T$. It is easy to see that T is indeed a triangulation. Furthermore, the number of vertices of T is

$$|T_1| + \sum_{\ell=2}^{k}(|T_\ell| - 1) = |C_1| + 1 + \sum_{\ell=2}^{k}|C_\ell| = |C|$$

while the number of external vertices of T is

$$1 + \sum_{\ell=1}^{k}i_\ell + 1 = t_1(C) + 1.$$

We have thus defined ω; in particular, writing δ for the function sending $((T_1, i_1), \ldots, (T_k, i_k))$ to T, we have $\omega = \delta \circ \omega \circ \alpha$ (where ω acts on a tuple of diagram-integer pairs in the obvious way). It remains only to show that ω is a bijection. To that purpose, it suffices to define a unique decomposition γ of a triangulation T reversing the above construction, that is, inverting δ. This follows from the observation that

$$\beta \circ \omega^{-1} \circ \gamma = \alpha^{-1} \circ \omega^{-1} \circ \delta^{-1} = (\delta \circ \omega \circ \alpha)^{-1} = \omega^{-1},$$

so we automatically get a recursively-defined inverse of ω. So, let T be a triangulation and $v_0, v_1, \ldots, v_i$ be the exterior vertices of T read counterclockwise with $v_0 v_i$ the root edge. Again reading counterclockwise, vertex v_i has two or more external neighbors $v_0, v_{i_1}, v_{i_2}, \ldots, v_{i_{k-1}}, v_{i_k}$. Then deleting all edges incident to v_i leaves a sequence of unrooted triangulations $T_1, \ldots, T_k$ pairwise joined at vertices $v_{i_1}, \ldots, v_{i_{k-1}}$ (see Figure 6.1). Root each T_ℓ at the unique edge incident to $v_{i_{\ell-1}}$ which was previously incident to a bounded face, where $i_0 = 0$. Then it readily follows that setting $\gamma(T) = ((T_1, i_1), \ldots, (T_k, i_k))$ gives the desired decomposition; T_ℓ has exactly $i_\ell + 1$ exterior vertices and, furthermore, clearly $\delta(\gamma(T)) = T$. This concludes the proof. $\qquad\square$

Both our bijection between connected top-cycle-free diagrams and triangulations and the bijection of Courtiel, Yeats, and Zeilberger between planar bridgeless maps and connected top-cycle-free diagrams are recursively-defined. Obtaining a direct bijection mapping connected top-cycle-free diagrams to these other objects remains open.

7. The bijection ψ

In order to understand the solution (5.2) to the binomial tree-like equation, Courtiel and Yeats [CY17] investigated the asymptotics of the parameters defining the solution, including the index of the first terminal chord, the number of terminal chords, and the differences between the indices of consecutive terminal chords in the intersection order. For the former they obtained a recurrence relation for the number $c_{n,k}$ of connected diagrams with n chords such that $t_1 \geqslant n - k$. In addition to recursively computing the associated exponential generating function and estimating the asymptotics of $c_{n,k}$, they used this result to derive the following count.

Theorem 7.1 (Courtiel and Yeats [CY17, Corollary 11]). *The number of connected diagrams with n chords and exactly one terminal chord is $(2n - 3)!!$.*

This is the same as the number of (arbitrary) diagrams of size n. Courtiel and Yeats obtained this count inductively by removing the root chord, similar to arguments we employed in Section 3. In this section we describe and study a bijection between the set $\mathcal{T}_{n+1}$ of 1-terminal diagrams with $n+1$ chords and the set $\mathcal{D}_n$ of diagrams with n chords. This map was actually first discovered by Yeats almost a decade ago in the course of the original work with Marie [MY13] on chord diagram generating series solutions to Dyson–Schwinger equations, but never published or, to our knowledge, significantly studied.[1] Yeats used a recursive formulation related

---

[1]Personal communication.

to the inductive proof of Theorem 7.1; here we describe and concentrate on a new, simpler formulation. We will briefly return to Yeats' formulation in Section 7.2 in the context of Stirling permutations.

Theorem 7.2. *There is a bijection $\psi\colon \mathcal{T}_{n+1} \to \mathcal{D}_n$ between 1-terminal diagrams of size $n+1$ and diagrams of size n. Furthermore, the bijection*

   (i) preserves nestings,

  (ii) reduces the number of crossings by n,

 (iii) restricts to a bijection between connected nonnesting diagrams of size $n+1$ and nonnesting diagrams of size n, and

 (iv) restricts to a bijection between 1-terminal top-cycle-free diagrams of size $n+1$ and noncrossing diagrams of size n.

Proof. Consider $T \in \mathcal{T}_{n+1}$ with chords $c_1 < c_2 < \cdots < c_{n+1}$ in the standard order (which agrees with the intersection order by 1-terminality). All but the last point of T partition into a sequence of source-sink groups, one for each source of T. Recall that, since T is 1-terminal, these groups only contain the source and maximal interval of sinks immediately following the source. Then we define $\psi(T)$ to be the diagram obtained by

   (1) moving each source to the end of its source-sink group, and

   (2) deleting the formerly terminal chord c_n.

Figure 7.1 displays a representative example of T and $\psi(T)$. Note that the bijection ψ induces a mapping, given by the construction, between the chords of T and the chords of its image $\psi(T)$. We can therefore abuse notation and write $\psi(c)$ for the image of a non-terminal chord c under this induced mapping.

Step (1) converts all but the last source-sink group in T into a corresponding *sink-source group* in $\psi(T)$, consisting of a source together with the maximal interval of sinks adjacent to the source on the left. Observe that we can also dually characterize this as uncrossing each non-terminal chord c with its rightmost right neighbor c' by moving the source of c' immediately ahead of the sink of c while maintaining the relative order of all other endpoints. In particular, the following key property holds.

Claim 7.3. *A non-terminal chord $c \in T$ has k right neighbors if and only if $\psi(c)$ has $k-1$ right neighbors.*

This gives property (ii). Observe that for non-terminal chords $c, c' \in T$, c' is nested under c if and only if $\psi(c')$ is nested under $\psi(c)$ by the construction of ψ. Since the terminal chord is necessarily not part of any nestings we infer property (i).

Now clearly the codomain of ψ is $\mathcal{D}_n$, so to prove that ψ is a bijection between the designated sets it suffices to exhibit its inverse. To that end, let $D \in \mathcal{D}_n$ and define $\phi(D)$ to be the diagram obtained by
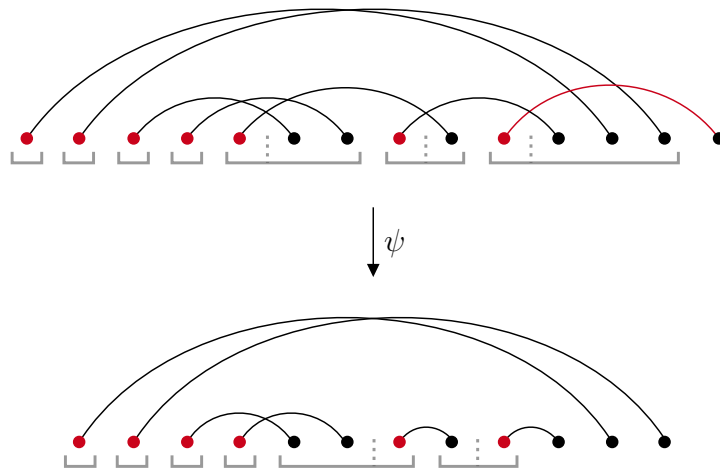
Figure 7.1: An example of a 1-terminal diagram and its image diagram under the bijection ψ. The source-sink groups "flipped" into sink-source groups by ψ are indicated by the horizontal brackets, with the "flip axes" indicated by the dotted lines, and the sources and terminal chord of T are highlighted.

$(1')$ concatenating a single chord to the end of D, and

$(2')$ moving the source of each sink-source group to the beginning of its sink-source group.

Note that we could also skip using $(2')$ on the terminal chord and instead of $(1')$ directly add a chord covering the rightmost maximal interval of sinks. It is readily apparent that $(1')$ and $(2')$ invert (2) and (1), respectively, implying that ϕ is the inverse of ψ.

It remains only to prove properties (iii) and (iv). For the former, Corollary 3.10 implies that connected nonnesting diagrams are 1-terminal, so the property follows by nesting preservation. For the latter, property (iv), we require a structural characterization of 1-terminal top-cycle-free diagrams. Recall that T is 1-terminal.

Claim 7.4. *Diagram T is top-cycle-free if and only if T is a tree[2] and every non-terminal chord has exactly one right neighbor.*

Proof. The "if" direction trivially holds. For the other direction, assume T is top-cycle-free. Note that bottom cycle diagrams have chords with two right neighbors, so it suffices to show that every non-terminal chord has exactly one right neighbor (since T consequently must be a tree). If not, then there exists non-terminal $c \in \mathcal{T}$ with at least two right neighbors d and d'. Since T is top-cycle-free d and d' do not cross and we may assume that d is nested under d'. Choose e as far right as possible such that there is a nonnesting d-e path nested under d'. Then either e has a right neighbor crossing d', in which case T contains a top cycle subdiagram, or e is terminal. In either case we get a contradiction. $\qquad\square$

---

[2]That is, $G(T)$ is a tree.

Note that we could also obtain this claim using a quicker induction argument, but the above proof offers more insight. It in particular reflects the fact that bottom cycle diagrams are not 1-terminal.

To obtain property (iv), suppose T is top-cycle-free. Then it follows by Claims 7.4 and 7.3 that each chord in the image $\psi(T)$ has no right neighbors, implying that there are no crossings at all. We can similarly infer that for each noncrossing diagram D every non-terminal chord in $\psi^{-1}(D)$ has exactly one right neighbor, as required. $\square$

Among other things, this sheds further light on the consequence of Theorem 6.1 that 1-terminal top-cycle-free diagrams are in bijection with triangulations with no interior vertices and, therefore, are counted by the Catalan numbers. In a nutshell, (iv) implies that we can think of 1-terminal top-cycle-free diagrams as the connectivity 1 equivalent to noncrossing diagrams, since trees have connectivity 1. As indicated by Claim 7.4, they are also minimally 1-terminal in the sense that each chord has the minimum number of right neighbors required to be 1-terminal.

7.1. Higher terminality

In this section, we define a generalization of terminal chords and 1-terminal diagrams which is analogous to the generalization of k-connectedness from connectedness. We then specifically study the relation between k-terminality and the bijection ψ.

Definition 7.5 (k-terminal chords and diagrams)**.** Let C be a chord diagram. For $k \in \mathbb{N}$, a chord $c \in C$ is k-*terminal* if it is incident to at most $k-1$ outgoing edges in $G(C)$, that is, it has at most $k-1$ right neighbors. We extend this language to diagrams: C is k-*terminal* if there is no j-terminal chord before the jth-to-last chord for all $1 \leqslant j \leqslant k$. Furthermore, the *terminality of* C is k if C is k-terminal but not $(k+1)$-terminal.

As expected, for chords '1-terminal' is simply another name for 'terminal'. Since the chord with rightmost sink in each connected component is necessarily terminal, it follows immediately from the definition that k-terminal diagrams are connected and the last $k+1$ chords form a clique; in particular, there are exactly j j-terminal chords for all $1 \leqslant j \leqslant k$. Furthermore, clearly k-terminal chords and diagrams are also j-terminal for $1 \leqslant j \leqslant k$.

With the observations at the end of the previous section in mind, we can generalize statement (iv) of Theorem 7.2 to get a connectivity k equivalent to noncrossing diagrams. Call a diagram C k-*terminal-minimal* if all but its last $k-1$ chords have exactly k right neighbors. Clearly C is k-terminal and furthermore, in particular, 1-terminal top-cycle-free diagrams are 1-terminal-minimal. We will require a basic fact about connectivity, followed by two important statements about the relationship between k-connectivity, k-terminality, and ψ. For a simple graph G, write $G[A]$ for the induced subgraph on $A \subseteq V(G)$ and $\delta_{G-A}(A)$ for the minimum number of neighbors that a vertex in A has in $G - A$.

Lemma 7.6. *If (i) $G - A$ is k-connected, (ii) $G[A]$ is either k-connected or has size at most k, (iii) $\delta_A(V(G) - A) \geqslant \min\{k, |A|\}$, and (iv) $\delta_{G-A}(A) \geqslant k$, then G is k-connected.*

We omit the straightforward proof of this fact.

Proposition 7.7. *If diagram C is k-terminal and has at least $k+1$ chords then it is k-connected.*

Proof. Let c be the root chord of a k-terminal diagram C of size at least $k+1$. By definition $C-c$ is k-terminal, so it is either the complete diagram of size k or we may inductively assume that it is k-connected. In the former case C is also complete and thus k-connected, while in the latter case the fact that c has k right neighbors in C implies that C is k-connected by Lemma 7.6 with $A = \{c\}$. $\qquad\square$

Proposition 7.8. *The map ψ restricts to a bijection between k-terminal diagrams of size n and $(k-1)$-terminal diagrams of size $n-1$.*

Proof. As with (iv) of Theorem 7.2, this is a straightforward consequence of Claim 7.3. $\qquad\square$

We similarly get our desired conclusion.

Proposition 7.9. *The map ψ restricts to a bijection between k-terminal-minimal diagrams of size n and $(k-1)$-terminal-minimal diagrams of size $n-1$.*

Corollary 7.10. *The map ψ^k on k-terminal diagrams restricts to a bijection between k-terminal-minimal diagrams of size $n+k$ and noncrossing diagrams of size n. In particular, k-terminal-minimal diagrams are counted by the Catalan numbers.*

While Claim 7.4 provides a structural characterization of 1-terminal-minimality, we have yet to obtain such a characterization for k-terminal-minimality. Our preliminary investigations indicate though that there should be a similar description in terms of k-terminal diagrams forbidding an infinite class of subdiagrams.

Conjecture 7.11. There is a "nice" infinite forbidden subdiagram characterization of k-terminal-minimality.

In his infamous compilation of combinatorial objects counted by the Catalan numbers, Stanley [Sta13] used ballot sequences and functions $f : \mathbb{N} \to \mathbb{N}$ satisfying $f(i) \leqslant i$ for all i to define $2^{\aleph_0}$ chord diagram interpretations of the Catalan numbers $\{C_n\}_{n \geqslant 0}$. The noncrossing and nonnesting diagrams are recovered by setting $f(i) = 1$ and $f(i) = i$, respectively, so in a sense these interpretations lie between the two. Yet this construction only gives a finite number of interpretations for any fixed size n. With the set of k-terminal-minimal diagrams we have provided a countable infinity of combinatorial interpretations of C_n. Furthermore, combining Stanley's construction together with the map ψ gives $2^{\aleph_0}$ combinatorial interpretations of the Catalan numbers with $\aleph_0$ interpretations at each fixed n.

We now turn to generalizing statement (iii) of Theorem 7.2. The proof used the fact that connectivity is equivalent to 1-terminality for nonnesting diagrams. This actually points to a more general statement about nonnesting diagrams.

Proposition 7.12. *A nonnesting diagram is k-connected if and only if it is k-terminal and has at least k chords.*
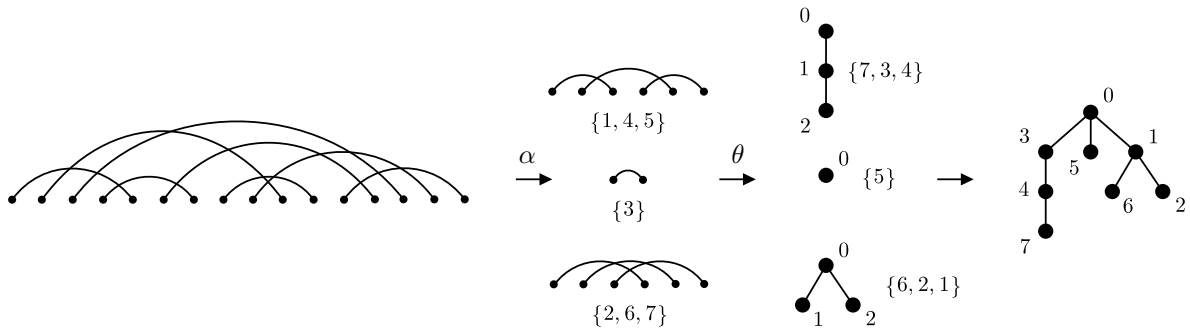
Figure 7.2: An example of the recursive construction of the image increasing tree $\theta(C)$ of a 1-terminal diagram C under the bijection θ.

Proof. By Proposition 7.7 it suffices to prove the "only if" direction. Let C be nonnesting and k-connected and c be its root chord. By the Erdős–Szekeres theorem the left and right neighborhoods of each chord of C form cliques, implying by k-connectivity that the neighborhood of c is a clique of size at least k. It follows that c cannot be part of any minimal vertex cut, so $C - c$ is either complete or k-connected. In the former case we are done, while in the latter case we inductively get that $C - c$ is k-terminal, so C is as well. $\qquad\square$

Combining this observation with Theorem 7.2 and Proposition 7.8, we get the following.

Corollary 7.13. *The map ψ restricts to a bijection between k-connected nonnesting diagrams of size n and $(k-1)$-connected nonnesting diagrams of size $n-1$.*

Corollary 7.14. *The map ψ^k restricts to a bijection between k-connected nonnesting diagrams of size $n+k$ and nonnesting diagrams of size n. In particular, k-connected nonnesting diagrams are counted by the Catalan numbers.*

7.2. Relationship with other double factorial objects

Recall that there are a number of other classical combinatorial objects counted by the double factorials $(2n-1)!!$ in addition to chord diagrams. We will briefly focus on two of the most notable: increasing ordered trees and Stirling permutations. A (rooted) tree T of size n is *ordered* or *plane* if it is equipped with a total ordering of the children of each vertex $v \in T$. The tree T is *increasing* if its vertices are labelled with the integers $0, 1, 2, \ldots, n-1$ such that the label of any child is greater than its parent. A *Stirling permutation* of size n is a permutation of the multiset $\{1, 1, 2, 2, \ldots, n, n\}$ such that, for all i, all values between the two occurrences of i are greater than i. Stirling permutations were introduced by Gessel and Stanley to give a combinatorial interpretation to the Stirling polynomials. They have since been studied extensively and generalized in multiple different ways (see e.g. [GS78, BÓ9, Jan08, JKP11]), as have increasing ordered trees (see e.g. [BFS92, PP07]). Write $\mathcal{S}_n$ and $\mathcal{I}_n$ for the sets of Stirling permutations and increasing ordered trees of size n, respectively.

There are classic recursive constructions of both $\mathcal{C}_n$ and $\mathcal{S}_n$: insert a root chord and insert nn into each element of $\mathcal{C}_{n-1}$ and $\mathcal{S}_{n-1}$, respectively, in all possible ways. Since there
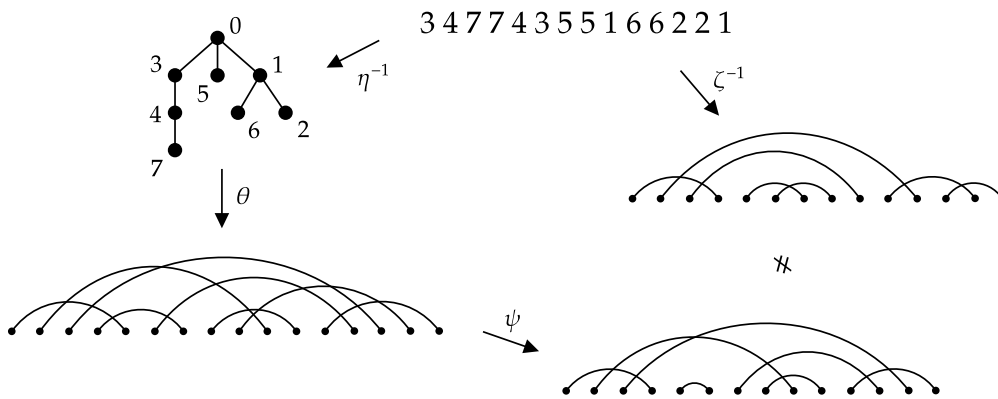
Figure 7.3: A Stirling permutation σ such that $\zeta^{-1}(\sigma) \neq (\psi \circ \theta \circ \eta^{-1})(\sigma)$.

are always $2n - 1$ possible insertion places, this proves that both of these sets have cardinality $(2n - 1)!!$ and gives a recursively-defined bijection ζ between them. This leads into a simple characterization of 1-terminality and the bijection ψ on Stirling permutations.

Proposition 7.15. *Diagram C is 1-terminal if and only if $\zeta(C)$ begins with 1 and ends with 1. In this case, $\zeta(\psi(C))$ is obtained from $\zeta(C)$ by removing both occurrences of 1 and normalizing the alphabet.*

Proof. Consider a diagram C of size n and let C' be obtained by removing the root chord c of C. Since the result clearly holds if C is simply a single chord, we may assume it has at least two chords and that the first statement holds for all smaller diagrams. If C is 1-terminal then C' is also 1-terminal and the sink of the root chord is neither placed at the front nor the end of C', implying that nn is placed after the first element of $\zeta(C')$ and before the last element of $\zeta(C')$. But those elements are 1, so they are also 1 in $\zeta(C)$. This argument is easily reversed, giving the first statement. For the second statement, observe that $\psi(C') = \psi(C) - \psi(c)$ (since the source-sink group of c has no sinks) and $\zeta(C') = \zeta(C) - nn$. Then the result follows straightforwardly from induction. $\square$

The classic bijection η between increasing ordered trees and Stirling permutations sends trees of size $n + 1$ to permutations of size n: for a tree $T \in \mathcal{I}_{n+1}$, delete the root label and transfer the remaining labels from vertices to parent edges, then take a pre-order traversal around the tree, traversing each edge twice. The encountered sequence of labels is the Stirling permutation $\eta(T)$.

As hinted at prior in the paper, and from the fact that there are $(2n - 1)!!$ increasing ordered trees of size $n + 1$, the decomposition from Section 4 defined by the maps α and β recursively defines a natural bijection θ between the set $\mathcal{T}_{n+1}$ of 1-terminal diagrams and the set $\mathcal{I}_{n+1}$ of increasing ordered trees. For each $C \in T_{n+1}$, apply α to get the 1-terminal subdiagrams $C_1, \ldots, C_k$ and intervals $I_1, \ldots, I_k$ of $[1, n]$. Then recursively apply θ to $C_1, \ldots, C_k$ to get increasing ordered trees $T_1, \ldots, T_k$, graft them to a new root of label 0 in that order, and finally apply a reverse-order-preserving bijection to reassign each subtree T_ℓ with the labels from I_ℓ. The resulting increasing ordered tree T is then set as the image of C under θ. An example of this

construction is given in Figure 7.2. We omit the proof that this actually defines a bijection between $\mathcal{T}_{n+1}$ and $\mathcal{I}_{n+1}$; it proceeds similarly to the proof of Theorem 6.1. Then, in this context, ψ plays the role of extending this to a bijection to chord diagrams of size n. We used a reverse-order-preserving bijection on the labels to define θ because this gives a simple non-recursive construction for θ: writing $c_1 < c_2 < \cdots < c_{n+1}$ for the chords of $C \in \mathcal{T}_{n+1}$, let T be the tree with vertices labeled $1, 2, \ldots, n+1$ and the children of vertex i are $(i_1, \ldots, i_k)$, where c_{i_j} is the chord attached to the jth sink in the source-sink group of c_i. The labels of the resulting tree T are decreasing, so we replace each label i with $n + 1 - i$ to get the increasing ordered tree $\theta(C)$. We started with the recursive construction to highlight the role our main recursive decompositions from Section 4.

From all of the above we get two bijections between Stirling permutations of size n and chord diagrams with n chords: ζ^{-1} and $\psi \circ \theta^{-1} \circ \eta^{-1}$. These bijections are highly distinct, typically mapping a given Stirling permutation to two different diagrams; e.g. see Figure 7.3. We can think of ζ^{-1} as encoding the *recursive view* of chord diagrams and $\psi \circ \theta^{-1} \circ \eta^{-1}$ as encoding the *tree structure view* of chord diagrams. In light of Proposition 7.15 one can think of the map ψ as playing a role in both perspectives, forming a kind of bridge translating 1-terminality from the recursive view to the tree structure view.

8. Conjectures and conclusions

For a fixed set $\mathcal{X}$ of diagrams, let $\mathcal{D}_n(\mathcal{X})$ be the set of chord diagrams of size n with no subdiagram lying in $\mathcal{X}$ and set $\mathcal{C}_n(\mathcal{X}) = \mathcal{D}_n(\mathcal{X}) \cap \mathcal{C}$, the connected $\mathcal{X}$-*free* diagrams. Writing T_i for the top cycle diagram of size i, note that $\mathcal{C}_n(\{\})$ is of course $\mathcal{C}_n$, the set of size n connected diagrams, and $\mathcal{C}_n(T_{\geqslant 3})$ is exactly $\mathcal{C}_{top}$, the set of size n connected top-cycle-free diagrams.

Forbidding certain subdiagrams has previously been studied in the literature. Much past work has focused on forbidding complete subdiagrams K_k and *nesting subdiagrams* N_k of size k, traditionally referred to as k-*crossings* and k-*nestings* (see Figure 8.1). It is well known that noncrossing diagrams $\mathcal{D}_n(K_2)$ and nonnesting diagrams $\mathcal{D}_n(N_2)$ are both counted by the Catalan numbers. Following work by Touchard [Tou52], Riordan [Rio75], and de Sainte-Catherine [dSC83] on the distribution of 2-crossings and 2-nestings, Gouyou-Beauchamps [GB89] studied the enumeration of N_3-free diagrams via involutions with no decreasing sequence of length 6, essentially giving a bijection between such diagrams and pairs of noncrossing Dyck paths. A *Dyck path* of size n is a lattice path of North and East steps from $(0,0)$ to (n, n). Noncrossing Dyck paths form a distributive lattice $\mathcal{L}_n^S$ known as the nth *Stanley lattice*. De Sainte-Catherine and Viennot [dSCV86] proved that

$$C_n C_{n+2} - C_{n+1}^2 = \frac{6}{(n+1)(n+1)^2(n+3)} \binom{2n}{n} \binom{2n+2}{n+1}$$

is the number of intervals of $\mathcal{L}_n^S$. Chen et al. [CDD$^+$07] extended this early work to k-crossings and k-nestings, proving that their maximum size in a diagram defines a pair of symmetrically distributed statistics and therefore $|\mathcal{D}_n(K_k)| = |\mathcal{D}_n(N_k)|$. In particular, via a bijection between partitions and vacillating tableaux underlying their results they obtained the following.

Figure 8.1: The complete diagram and nesting diagram; the former is the unique representative of a complete graph.

Theorem 8.1 (Chen et al. [CDD$^+$07])**.** *The numbers of K_k-free and N_k-free diagrams of size n are equal to the number of closed lattice paths of length $2n$ in the set*

$$\{(a_1, a_2, \ldots, a_{k-1}) \mid a_1 \geqslant a_2 \geqslant \cdots \geqslant a_{k-1} \geqslant 0, a_i \in \mathbb{Z}\}$$

from the origin to itself with units steps in any coordinate direction or its negative.

Let $\mathrm{Int}(P)$ denote the set of all intervals of a poset P.

Corollary 8.2 (Gouyou-Beauchamps [GB89], Chen et al. [CDD$^+$07])**.** *There is a bijection between $\mathcal{D}_n(K_3)$ and $\mathrm{Int}(\mathcal{L}_n^S)$, so both have cardinality $C_n C_{n+2} - C_{n+1}^2$.*

While the language we use here is inspired by graph theory and, in particular, the graph-theoretic nature of top cycle diagrams, classically in enumerative combinatorics the forbidding of substructures takes the form of pattern avoidance. Inspired by the broad literature on pattern avoidance in permutations (see [Kit11]), several authors have defined and studied pattern avoidance in set partitions and matchings, that is, chord diagrams [Kla96, Jel07, Sag10, BE13]. Our definition of forbidding subdiagrams in particular matches the definitions of Jelínek [Jel07] and Sagan [Sag10] of avoiding matching patterns. Following Chen et al., Jelínek considered forbidding other subdiagrams of size three: $D_{231} = \{(1,5), (2,6), (3,4)\}$, $D_{312} = \{(1,6), (2,4), (3,5)\}$, $D_{213} = \{(1,5), (2,4), (3,6)\}$, and $D_{132} = \{(1,4), (2,6), (3,5)\}$. These are *permutation diagrams*, so called because they are defined (and indexed) by the permutation determined by their sinks (see Figure 8.2). Jelínek constructed bijections between $\mathcal{D}_n(K_3)$ and $\mathcal{D}_n(D_{231})$ and between $\mathcal{D}_n(D_{213})$ and $\mathcal{D}_n(D_{132})$ preserving certain substructures. For the latter, he actually passed through top-cycle-free diagrams, giving bijections between both of those sets and $\mathcal{D}_n(T_{\geqslant 3})$. Bloom and Elizalde [BE13] later enumerated these classes of diagrams, simplifying prior bijections and deriving the algebraic generating function of $\mathcal{D}_n(D_{213})$ and, thereby, $\mathcal{D}_n(D_{132})$ and $\mathcal{D}_n(T_{\geqslant 3})$.

The combinatorial significance of top cycle diagrams motivates considering other diagrams with graph-theoretic relevance and, in particular, studying sets of diagrams which forbid such graphical subdiagrams. In graph theory, graphs forbidding certain cycles as induced subgraphs are of great interest. Most notably this includes triangle-free graphs (forbidding a cycle of size 3), forests (forbidding all cycles), chordal graphs (forbidding cycles of size 4 or greater), and bipartite graphs (forbidding odd size cycles). By forbidding the corresponding top and bottom cycles, we get the chord diagram versions of each of these graph classes, namely $\mathcal{D}_n(T_3)$, $\mathcal{D}_n(T_{\geqslant 3}, B_{\geqslant 3})$,
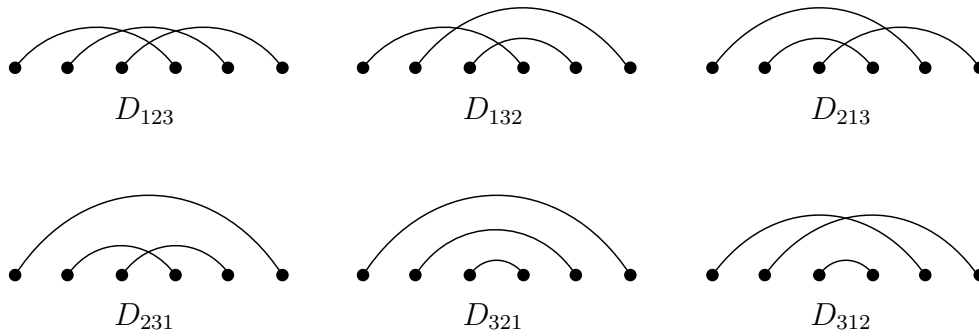
Figure 8.2: The six permutation diagrams of size 3.

$\mathcal{D}_n(T_{\geqslant 4}, B_{\geqslant 4})$, and $\mathcal{D}_n(\{T_{2k+1}, B_{2k+1}\}_{k\geqslant 1})$, where B_i is the bottom cycle diagram of size i.[3] In addition to the top-cycle-free diagrams $\mathcal{D}_n(T_{\geqslant 3})$, we naturally also consider bottom-cycle-free diagrams $\mathcal{D}_n(B_{\geqslant 3})$.

As discussed previously, we already know that triangle-free diagrams $\mathcal{D}_n(T_3)$ are in bijection with, among other things, intervals $\mathrm{Int}(\mathcal{L}_n^S)$ of the Stanley lattice (Corollary 8.2). Tamari [Tam62] defined a partial order on the set $\mathcal{B}_n$ of plane binary trees with n non-leaf vertices and proved that it specified a lattice, the nth *Tamari lattice* $\mathcal{L}_n^T$, with a tree operation known as right rotation as the covering relation. Chapoton [Cha06] proved that the cardinality of $\mathrm{Int}(\mathcal{L}_n^T)$ is given by (6.2); later, Bernardi and Bonichon [BB09] provided a bijection between Tamari intervals and triangulations explaining their common count. Along with a bijection between triangulations and bridgeless planar maps, Fang [Fan18] obtained a bijection between bridgeless planar maps and Tamari intervals; all of these bijections passed through so-called "sticky trees". It follows from these results and Theorem 6.1 that connected top-cycle-free diagrams $\mathcal{C}_n(T_{\geqslant 3})$ are equinumerous with intervals of the $(n-1)^{\text{th}}$ Tamari lattice.

Corollary 8.3. *There is a bijection between $\mathcal{C}_n(T_{\geqslant 3})$ and $\mathrm{Int}(\mathcal{L}_{n-1}^T)$, so both have cardinality $\frac{2}{n(n-1)}\binom{4n-3}{n-2}$.*

As with noncrossing and nonnesting diagrams, Dyck paths and plane binary trees are well known to be counted by the Catalan numbers. There are two other notable so-called *Catalan posets* constructed on a groundset counted by the Catalan numbers: the nth Kreweras lattice $\mathcal{L}_n^K$, defined by ordering the set of noncrossing partitions of the set $[n]$ by refinement, and the nth Pallo comb poset PC_n refining the Tamari lattice. Kreweras [Kre72] and Pallo [Pal03] proved that the intervals of these lattices are counted by

$$\frac{1}{2n+1}\binom{3n}{n}$$

and the coefficients of the generating series $C(xC(x))$, respectively, where $C(x) = \frac{1-\sqrt{1-4x}}{2x}$ is the generating function of the Catalan numbers. By using bijections between Catalan objects to define the three lattices on a common groundset (e.g. Dyck paths [BB09]), it can be shown that

---

[3]Note that $B_3 = T_3$.

the Stanley lattice $\mathcal{L}_n^S$ is an extension of the Tamari lattice $\mathcal{L}_n^T$ which itself is an extension of the Kreweras lattice $\mathcal{L}_n^K$. From the above two corollaries, the fact that the Stanley lattice extends the Tamari lattice reflects the trivial observation that $C_n(T_{\geqslant 3})$ is a subset of $D_n(T_3)$.

Each of these three Catalan lattices has been the subject of extensive study throughout mathematics, with interest and applications in enumerative combinatorics (e.g. [BMCPR13]) and a diversity of other disciplines. Most notably, Defant [DEM20] recently obtained a number of bijections between the intervals of Catalan posets and certain pattern-avoiding *uniquely sorted* permutations, those that have exactly one preimage under West's classic stack-sorting map [Knu73, Wes90]. Letting $\mathcal{U}_n(\tau^{(1)}, \ldots, \tau^{(r)})$ denote the set of uniquely sorted permutations in $\mathcal{U}_n$ that avoid the patterns $\tau^{(1)}, \ldots, \tau^{(r)}$, Defant found bijections between

- $U_{2n+1}(321)$ and $\mathrm{Int}(\mathcal{L}_n^S)$,

- $U_{2n+1}(132)$ and $\mathrm{Int}(\mathcal{L}_n^T)$,

- $U_{2n+1}(312, 1342)$ and $\mathrm{Int}(\mathcal{L}_n^K)$,

- $U_{2n+1}(231, 4132)$ and $\mathrm{Int}(\mathrm{PC}_n)$, and

- each of $U_{2n+1}(321)$, $U_{2n+1}(132, 312)$, $U_{2n+1}(132, 312)$, $U_{2n+1}(231, 312)$, and $\mathrm{Int}(\mathcal{A}_n)$,

the last of which is the intervals of the Catalan antichain $\mathcal{A}_n$.

If we further exclude bottom cycles, we get the tree diagrams $C_n(T_{\geqslant 3}, B_{\geqslant 3})$; comparing manual calculations of their count for small n with OEIS sequence A001764 [SI22], we conjecture the following.

Conjecture 8.4. There is a bijection between $C_n(T_{\geqslant 3}, B_{\geqslant 3})$ and $\mathrm{Int}(\mathcal{L}_{n-1}^K)$, so both have cardinality $\frac{1}{2n-1}\binom{3n-3}{n-1}$.

This conjecture was recently proved by the author in [Nab22] via a structural decomposition of tree diagrams. It is notable that to pass from the Stanley case to the Tamari case we exclude an infinite set of cycle diagrams *and* assert connectedness, while to further pass to the Kreweras case we need only further exclude another infinite set of cycle diagrams. This may reflect a closer relationship between the Tamari and Kreweras lattices than between the Stanley and Tamari lattices, as is also suggested by the Dyck path realizations of these lattices given by Bernardi and Bonichon [BB09] (see their work for details).

Manual calculations similarly indicate that connected chordal diagrams $\mathcal{C}_n(T_{\geqslant 4}, B_{\geqslant 4})$, bipartite diagrams $\mathcal{C}_n(\{T_{2k+1}, B_{2k+1}\}_{k\geqslant 1})$, and bottom-cycle-free diagrams $\mathcal{C}_n(B_{\geqslant 3})$ are enumerated by simple, combinatorially significant sequences.

Conjecture 8.5 (A001246). The cardinality of $\mathcal{C}_n(T_{\geqslant 4}, B_{\geqslant 4})$ is C_{n-1}^2.

Proposition 8.6 (A000264). *The cardinality of $\mathcal{C}_n(\{T_{2k+1}, B_{2k+1}\}_{k\geqslant 1})$ is the same as the set of all 3-edge-connected cubic planar loopless maps with $2n$ vertices and a distinguished Hamiltonian cycle.*
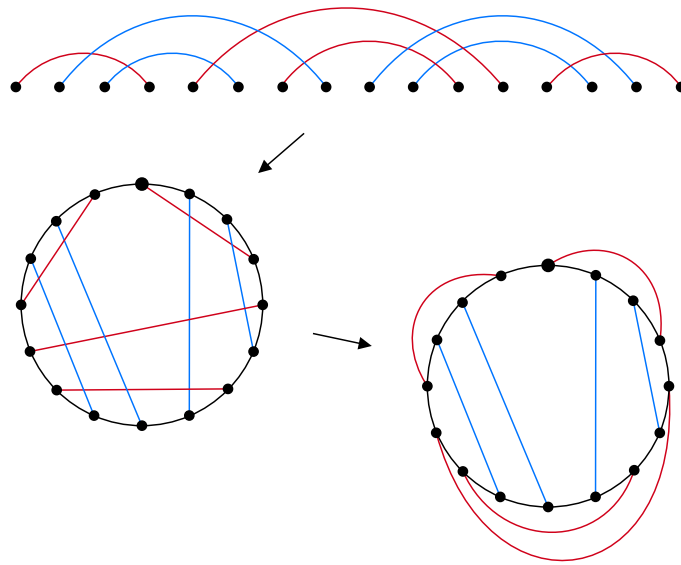
Figure 8.3: Transforming the representation of a connected bipartite diagram from its linear form to the circular form and then separating the color classes along the circle, yielding a 3-edge-connected rooted cubic planar loopless map. The root is indicated by the larger dot.

Conjecture 8.7 (A064062). The cardinality of $\mathcal{C}_n(B_{\geqslant 3})$ is

$$C(2; n-1) = \frac{1}{n-1} \sum_{k=0}^{n-2} \binom{2n-2}{n-2-k} \binom{n-2+k}{k}.$$

Neither of these three sets is equinumerous with the intervals of a known Catalan poset, although the possibility of such an association remains open for the latter two. The first conjecture clearly calls for a bijection between chordal diagrams of size n and ordered pairs of Catalan objects of size n. With regards to the second conjecture, Bloom and Elizalde [BE13] also enumerated diagrams forbidding a pair of permutation diagrams of size 3; in particular, they found that the *generalized Catalan numbers* $C(2; n)$ of Conjecture 8.7 also count $\{D_{213}, D_{132}\}$-free diagrams. This interestingly relates to the result of Jelínek [Jel07] that top-cycle-free diagrams are in bijection with D_{213}-free diagrams and D_{132}-free diagrams. It also further motivates our additional conjecture, informed by numerical evidence, that $|\mathcal{C}_n(B_{\geqslant 3})| \leqslant |\mathcal{C}_n(T_{\geqslant 3})|$ for all n. Nevertheless, Conjecture 8.7 was also recently resolved by the author and Mahmoud (see [Nab22, Section 3.1]) in the affirmative using a structural decomposition of bottom-cycle-free diagrams. As for the second statement, Proposition 8.6, the bijection to these maps is trivial: it can be readily verified that the circular representation of a connected bipartite diagram with one color class drawn within the circle and the other outside of the circle is a 3-edge-connected rooted cubic planar loopless map with the circle distinguishing the Hamiltonian cycle (see Figure 8.3).

All the enumerative conjectures we have made thus far have involved sets of connected diagrams. While none of their not-necessarily-connected versions have count sequences that appear on the OEIS, there is a classic functional equation relating the (ordinary) generating function

$D(x)$ of chord diagrams and the generating function $C(x)$ of connected chord diagrams,

$$D(x) = 1 + C(xD(x)^2).$$

Note that the empty diagram is not considered connected; see e.g. [FN00]. This is obtained by decomposing a diagram by the component containing the root chord and viewing the rest of the diagram as attached to the chords of that component. This straightforwardly generalizes to any class $\mathcal{D}(\mathcal{Z})$ determined by forbidding a fixed set $\mathcal{Z}$ of connected diagrams and its associated class of connected $\mathcal{Z}$-free diagrams $\mathcal{C}(\mathcal{Z})$. In particular, writing $G(x)$ and $F(x)$ for the generating functions of $\mathcal{D}(\mathcal{Z})$ and $\mathcal{C}(\mathcal{Z})$, we have

$$G(x) = 1 + F(xG(x)^2). \tag{8.1}$$

With a routine expansion this translates into the recurrence

$$a_n = \sum_{k=1}^{n} b_k \sum_{n_1 + \cdots n_{2k} = n-k} a_{n_1} \cdots a_{n_{2k}}, \tag{8.2}$$

where $a_n = [x^n]G(x)$ and $b_n = [x^n]F(x)$. In certain cases it may be possible to apply a formula for $F(x)$ or b_n and either (8.1) or (8.2) to obtain an explicit expression for $G(x)$ or a_n. Alternatively, it may feasible to use these equations to translate alternative combinatorial interpretations of $\mathcal{C}(\mathcal{Z})$ into a related combinatorial interpretation of $\mathcal{D}(\mathcal{Z})$.

The conjectured appearance of connectedness in the enumerative study of forbidden subdiagrams suggests that other notions of connectivity, in particular indecomposability and 1-terminality, may also find significance in this context. Note that none of the three notions of connectivity has a forbidden subdiagram characterization. As we mentioned in Section 6, indecomposable top-cycle-free diagrams are known to be in bijection with planar maps. We speculate that excluding other graphical diagrams may correspond to other natural types of combinatorial maps, but were not able to easily identify any such possible connections. On the other hand, applying 1-terminality seems to yield many new enumerative links. Write $\mathcal{T}_n(\mathcal{X})$ for the set of $\mathcal{X}$-free 1-terminal diagrams of size n. From Theorem 7.2 we have the following.

Corollary 8.8. *The cardinality of* $\mathcal{T}_n(T_{\geqslant 3}) = \mathcal{T}_n(T_{\geqslant 3}, B_{\geqslant 3})$ *is* C_{n-1}.

The enumeration of other such sets remains conjectural, based on manual calculations and sequence information on the OEIS.

Conjecture 8.9 (A117106). The cardinality of $\mathcal{T}_n(T_3)$ is the same as the set of semi-Baxter permutations of length $n-1$,

$$\frac{24}{(n-2)(n-1)^2 n(n+1)} \sum_{j=0}^{n-1} \binom{n-1}{j+2}\binom{n+1}{j}\binom{n+j+1}{j+1}.$$

Conjecture 8.10 (A001181). The cardinality of $\mathcal{T}_n(\{T_{2k+1}, B_{2k+1}\}_{k \geqslant 1})$ is the same as the set of Baxter permutations of length $n-1$,

$$\sum_{k=1}^{n-1} \frac{\binom{n}{k-1}\binom{n}{k}\binom{n}{k+1}}{\binom{n}{1}\binom{n}{2}}. \tag{8.3}$$

Conjecture 8.11 (A006318). The cardinality of $\mathcal{T}_n(B_{\geqslant 3})$ is the $(n-2)^{\text{nd}}$ Schröder number,

$$S_{n-2} = \sum_{k=0}^{n-2} C_k \binom{n-2+k}{n-2-k}.$$

See the work of Chung et al. [CGHK78] and Bouvel et al. [BGRR18] for definitions of Baxter and semi-Baxter permutations and proofs of the closed-form expressions for their counts. Note that semi-Baxter permutations are a relaxation of Baxter permutations, matching the fact that bipartite diagrams are triangle-free.

Clearly interesting enumerative structure seems to emerge from forbidding graphical subdiagrams and applying various notions of connectedness, warranting further study. In addition to cycles, excluding most notably complete graphs, trees, paths, and bipartite graphs has yielded structurally rich graph classes; forbidding their diagram representations may also find relevance in this context. Additionally, there are several natural questions that follow from Theorem 6.1. Are there bijections proving the above conjectures that translate between interesting statistics on the associated objects? For example, (8.3) is graded by the number of descents in the Baxter permutations, suggesting an associated statistic on 1-terminal bipartite diagrams. Finally, besides top-cycle-free diagrams does the inverse β preserve any other excluded subdiagram class of connected diagrams?

We solved tree-like equations involving a sequence of weights ϕ_k which arise in the solutions via valencies of the chords of a diagram. This closely relates to the weights which feature in the more physically-grounded work of Hihn and Yeats [HY19] and Courtiel, Yeats, and Zeilberger [CYZ19] on generalized Dyson–Schwinger equations. In the latter, these weights are cast as a product of binomial coefficients $\binom{\omega_i(C)+s-1}{\omega_i(C)}$ over all chords c_i in a diagram C, where $\omega_i(C)$ is a parameter known as the covering number of c_i and s is a positive integer. The covering number of c_i is defined as the number of intervals, that is, gaps between points of the diagram, assigned to c_i in a certain recursive covering procedure. One can readily see that these intervals correspond exactly to the intervals on either side of each of the m attachment points and components from Definition 3.12 of a chord of valency m; in other words, $\text{val}(c_i) = \omega_i(C) - 1$. So setting $\phi_k = \binom{k+s}{k+1}$ gives the weighted cases considered in prior work. Note though that [HY19] and [CYZ19] also simultaneously apply a separate weighting to the chords, so our work is not a full generalization of these studies, although it appears that such a generalization would readily go through using the methods of this paper; we left this for later work to maintain conciseness and focus. We additionally note that although this clarifies the relationship between Dyson–Schwinger equations considered in prior work and the tree-like equations studied here, it remains unclear whether tree-like equations in their full generality correspond to any meaningful physics. Though, as with prior work, if such a connection were made then the combinatorial solutions we obtained should prove useful in gaining new physical insight.

There are further generalizations of tree-like equations that arise by e.g. considering *systems* of combinatorial Dyson–Schwinger equations in certain *decorated* Connes–Kreimer Hopf algebras (see e.g. [Yea17, Nab22]). It would be of interest to study these generalizations; we speculate that such equations will likely have combinatorial solutions involving chord diagrams or closely related objects.

Several additional open questions remain. How exactly do the decompositions on chord diagrams developed here relate to the decompositions on certain leaf-labeled plane binary trees relied upon by Marie and Yeats [MY13]? Is there a suitably well-behaved generalization of the bijection ψ which acts on all connected diagrams and explains any of the enumerative results or connections discussed in this section or Section 6? We attempted at length to obtain such a bijection for Conjecture 8.7 but were thus far unsuccessful. Finally, we used the intersection order as the main chord ordering throughout this paper, in particular in Theorem 5.1. What about other orders, in particular the peeling order? Courtiel, Yeats, and Zeilberger [CYZ19, Proposition 41] proved that all of the necessary statistics are preserved by the peeling order, so our main theorem still holds under this replacement, but several of the proof ingredients, in particular Lemmas 5.3 and 5.4, do not straightforwardly translate because they rely on the connectedness of certain subdiagrams that may no longer be connected under the peeling order. It is likely that modest changes could be made to recover a related proof for a peeling version of Theorem 5.1.

Acknowledgements

References

[BÓ9] M. Bóna. Real zeros and normal distribution for statistics on Stirling permutations defined by Gessel and Stanley. *SIAM J. Discrete Math*, 23(1):401–406, 2009. `doi:10.1137/070702254`.

[BB09] O. Bernardi and N. Bonichon. Intervals in Catalan lattices and realizers of triangulations. *J. Combin. Theory Ser. A*, 116(1):55–75, 2009. `doi:10.1016/j.jcta.2008.05.005`.

[BE13] J. Bloom and S. Elizalde. Pattern avoidance in matchings and partitions. *Electron. J. Combin*, 20(2), 2013. `doi:10.37236/2976`.

[BFS92] F. Bergeron, P. Flajolet, and B. Salvy. Varieties of increasing trees. In J. C. Raoult, editor, *CAAP '92*, pages 24–48, Berlin, Heidelberg, 1992. Springer Berlin Heidelberg.

[BGRR18] M. Bouvel, V. Guerrini, A. Rechnitzer, and S. Rinaldi. Semi-Baxter and strong-Baxter: two relatives of the Baxter sequence. *SIAM J. Discrete Math*, 32(4):2795–2819, 2018. `doi:10.1137/17m1126734`.

[BLL98]   F. Bergeron, G. Labelle, and P. Leroux. *Combinatorial Species and Tree-like Structures, Encyclopedia of Mathematics and its Applications*, volume 67. Cambridge University Press, 1998.

[BMCPR13]   M. Bousquet-Mélou, G. Chapuy, and L.-F. Préville-Ratelle. The representation of the symmetric group on m-Tamari intervals. *Adv. Math*, 247:309–342, 2013. `doi:10.1016/j.aim.2013.07.014`.

[Bou94]   A. Bouchet. Circle graph obstructions. *J. Combin. Theory Ser. B*, 60(1):107–144, 1994. `doi:10.1006/jctb.1994.1008`.

[BR00]   B. Bollobás and O. Riordan. Linearized chord diagrams and an upper bound for Vassiliev invariants. *J. Knot Theory Ramifications*, 9(7):847–853, 2000. `doi:10.1142/s0218216500000475`.

[Bro64]   W. G. Brown. Enumeration of triangulations of the disk. *Proc. Lond. Math. Soc*, 3(14):746–768, 1964. `doi:10.1112/plms/s3-14.4.746`.

[CDD+07]   W. Y. C. Chen, E. Y. P. Deng, R. R. X. Du, R. P. Stanley, and C. H. Yan. Crossings and nestings of matchings and partitions. *Trans. Amer. Math. Soc*, 359(4):1555–1575, 2007. `doi:10.1090/s0002-9947-06-04210-3`.

[CGHK78]   F. R. K. Chung, R. L. Graham, E. Hoggatt, and M. Kleiman. The number of Baxter permutations. *J. Combin. Theory Ser. A*, 24:382–394, 1978. `doi:10.1016/0097-3165(78)90068-7`.

[Cha06]   F. Chapoton. Sur le nombre d'intervalles dans les treillis de Tamari. *Sém. Lothar. Combin*, 55, 2006.

[CK98]   A. Connes and D. Kreimer. Hopf algebras, renormalization and noncommutative geometry. *Comm. Math. Phys*, 199:203–242, 1998. `arXiv:hep-th/9808042`, `doi:10.1007/s002200050499`.

[CY17]   J. Courtiel and K. Yeats. Terminal chords in connected chord diagrams. *Ann. Inst. Henri Poincaré Comb. Phys. Interact*, 4(4):417–452, 2017. `arXiv:1603.08596`, `doi:10.4171/aihpd/44`.

[CY19]   J. Courtiel and K. Yeats. Next-to^k leading log expansions by chord diagrams. 2019. `arXiv:1906.05139`.

[CYZ19]   J. Courtiel, K. Yeats, and N. Zeilberger. Connected chord diagrams and bridgeless maps. *Electron. J. Combin*, 26(4), 2019. `doi:10.37236/7400`.

[DEM20]   C. Defant, M. Engen, and J. A. Miller. Stack-sorting, set partitions, and Lassalle's sequence. *J. Combin. Theory Ser. A*, 175, 2020. `doi:10.1016/j.jcta.2020.105275`.

[DM21]   J. Davies and R. McCarty. Circle graphs are quadratically χ-bounded. *Bull. Lond. Math. Soc*, 53(3):673–679, June 2021. `doi:10.1112/blms.12447`.

[dSC83]   M. de Sainte-Catherine. *Couplages et Pfaffiens en combinatoire, physique et informatique*. PhD thesis, University of Bordeaux, 1983.

[dSCV86]   M. de Sainte-Catherine and G. Viennot. Enumeration of certain Young tableaux with bounded height. *Lecture Notes in Math*, 1234:58–67, 1986. `doi:10.1007/bfb0072509`.

[Dug19]   W. Dugan. Sequences of trees and higher-order renormalization group equations. Master's thesis, University of Waterloo, 2019. URL: `http://hdl.handle.net/10012/14957`.

[Fan18]   W. Fang. Planar triangulations, bridgeless planar maps and Tamari intervals. *European J. Combin*, 70:75–91, 2018. `doi:10.1016/j.ejc.2017.12.002`.

[FN00]   P. Flajolet and M. Noy. Analytic combinatorics of chord diagrams. In *Formal Power Series and Algebraic Combinatorics*, pages 191–201. Springer, 2000.

[Foi08]   L. Foissy. Faá di Bruno subalgebras of the Hopf algebra of planar trees from combinatorial Dyson-Schwinger equations. *Adv. Math*, 218(1):136–162, 2008. `arXiv:0707.1204, doi:10.1016/j.aim.2007.12.003`.

[Foi10]   L. Foissy. Classification of systems of Dyson-Schwinger equations in the Hopf algebra of decorated rooted trees. *Adv. Math*, 224(5):2094–2150, 2010. `arXiv:0909.0358, doi:10.1016/j.aim.2010.01.024`.

[Foi14]   L. Foissy. General Dyson-Schwinger equations and systems. *Comm. Math. Phys*, 327(1):151–179, 2014. `arXiv:1112.2606, doi:10.1007/s00220-014-1941-0`.

[FS09]   P. Flajolet and R. Sedgewick. *Analytic Combinatorics*. Cambridge Univ. Press, Cambridge, 2009.

[Fus10]   E. Fusy. New bijective links on planar maps via orientations. *European J. Combin*, 31(1):145–160, 2010. `doi:10.1016/j.ejc.2009.02.008`.

[GB89]   D. Gouyou-Beauchamps. Standard young tableaux of height 4 and 5. *European J. Combin*, 10:69–82, 1989. `doi:10.1016/s0195-6698(89)80034-4`.

[GS78]   I. Gessel and R. P. Stanley. Stirling polynomials. *J. Combin. Theory Ser. A*, 24:24–33, 1978.

[HSS98]   I. Hofacker, P. Schuster, and P. F. Stadler. Combinatorics of RNA secondary structures. *Discrete Appl. Math*, 88(1–3):207–237, 1998. `doi:10.1016/s0166-218x(98)00073-0`.

[HY19]   M. Hihn and K. Yeats. Generalized chord diagram expansions of Dyson-Schwinger equations. *Ann. Inst. Henri Poincaré Comb. Phys. Interact*, 6(4):573–605, 2019. `doi:10.4171/aihpd/79`.

[Jan08]   S. Janson. Plane recursive trees, Stirling permutations and an urn model. *Fifth Colloquium on Mathematics and Computer Science*, pages 541–548, 2008. `doi:10.46298/dmtcs.3590`.

[Jel07]   V. Jelínek. Dyck paths and pattern-avoiding matchings. *European J. Combin*, 28:202–213, 2007. `doi:10.1016/j.ejc.2005.07.013`.

[JKP11]   S. Janson, M. Kuba, and A. Panholzer. Generalized Stirling permutations, families of increasing trees and urn models. *J. Combin. Theory Ser. A*, 118(1):94–114, 2011. `doi:10.1016/j.jcta.2009.11.006`.

[Kit11]   S. Kitaev. *Patterns in Permutations and Words*. Springer-Verlag, Berlin, 2011.

[Kla96]   M. Klazar. On $abab$-free and $abba$-free set partitions. *European J. Combin*, 17:53–68, 1996. `doi:10.1006/eujc.1996.0005`.

[Knu73]   D. E. Knuth. *The Art of Computer Programming, vol. 1, Fundamental Algorithms*. Addison-Wesley, 1973.

[KP13]   M. Kuba and A. Panholzer. A unifying approach for proving hook-length formulas for weighted tree families. *Graphs Combin*, 29:1839–1865, 2013. `doi:10.1007/s00373-012-1217-4`.

[Kre72]   G. Kreweras. Sur les partitions non croisées d'un cycle. *Discrete Math*, 1:333–350, 1972. `doi:10.1016/0012-365x(72)90041-6`.

[Kre98]   D. Kreimer. On the hopf algebra structure of perturbative quantum field theories. *Adv. Theor. Math. Phys*, 2(2):303–334, 1998. `arXiv:q-alg/9707029`, `doi:10.4310/atmp.1998.v2.n2.a4`.

[Mah22]   A. A. Mahmoud. Utilizing enumerative methods in quantum electrodynamics. 2022. `arXiv:2011.04291`.

[MY13]   N. Marie and K. Yeats. A chord diagram expansion coming from some Dyson-Schwinger equations. *Commun. Number Theory Phys*, 7(2):251–291, 2013. `arXiv:1210.5457`, `doi:10.4310/cntp.2013.v7.n2.a2`.

[Nab22]   L. Nabergall. *Enumerative perspectives on chord diagrams*. PhD thesis, University of Waterloo, 2022.

[Naj85]   W. Naji. Reconnaissance des graphes de cordes. *Discrete Math*, 54:329–337, 1985. `doi:10.1016/0012-365x(85)90117-7`.

[NW79]   A. Nijenhuis and H. Wilf. The enumeration of connected graphs and linked diagrams. *J. Combin. Theory Ser. A*, 27(3):356–359, 1979. `doi:10.1016/0097-3165(79)90023-2`.

[Pal03]   J. M. Pallo. Right-arm rotation distance between binary trees. *Inform. Process. Lett*, 87:173–177, 2003. `doi:10.1016/s0020-0190(03)00283-7`.

[Pan11]   E. Panzer. Hopf-algebraic renormalization of Kreimer's toy model. Master's thesis, Humboldt-Universität zu Berlin, 2011.

[PP07]   A. Panholzer and H. Prodinger. Level of nodes in increasing trees revisited. *Random Structures Algorithms*, 31(2):203–226, 2007. `doi:10.1002/rsa.20161`.

[PR14]   V. Pilaud and J. Rué. Analytic combinatorics of chord and hyperchord diagrams with k crossings. *Adv. Appl. Math*, 57:60–100, 2014. `doi:10.1016/j.aam.2014.04.001`.

[Rio75]   J. Riordan. The distribution of crossings of chords joining pairs of $2n$ points on a circle. *Math. Comp*, 29(129):215–222, 1975. `doi:10.2307/2005477`.

[Rot15]   L. Rotheray. Hopf subalgebras from green's functions. Master's thesis, Humboldt-Universität zu Berlin, 2015.

[Sag10]   B. E. Sagan. Pattern avoidance in set partitions. *Ars Combin*, 94:79–96, 2010.

[SE78]   P. R. Stein and C. J. Everett. On a class of linked diagrams, II. asymptotics. *Discrete Math*, 21(3):309–318, 1978. `doi:10.1016/0012-365x(78)90162-0`.

[SI22]   N. Sloane and The OEIS Foundation Inc. The on-line encyclopedia of integer sequences, 2022. URL: `http://oeis.org/`.

[Sta13]   R. P. Stanley. Catalan addendum, 2013. URL: `https://math.mit.edu/~rstan/ec/catadd.pdf`.

[Ste78]   P. R. Stein. On a class of linked diagrams, I. enumeration. *J. Combin. Theory Ser. A*, 24(3):357–366, 1978. `doi:10.1016/0097-3165(78)90065-1`.

[Tam62]   D. Tamari. The algebra of bracketings and their enumeration. *Nieuw Arch. Wiskd Ser. 3*, 10:131–146, 1962.

[Tou52]   J. Touchard. Sur un probleme de configurations et sur les fractions continues. *Canad. J. Math*, 4:2–25, 1952. `doi:10.4153/cjm-1952-001-8`.

[Tut62]   W. T. Tutte. A census of planar triangulations. *Canad. J. Math*, 14:21–38, 1962. `doi:10.4153/cjm-1962-002-9`.

[Wes90]   J. West. *Permutations with forbidden subsequences; and, Stack-sortable permutations*. PhD thesis, MIT, 1990.

[WL75]   T. R. S. Walsh and A. B. Lehman. Counting rooted maps by genus III: Nonseparable maps. *J. Combin. Theory Ser. B*, 18:222–259, 1975. `doi:10.1016/0095-8956(75)90050-7`.

[Wor80]   N. C. Wormald. A correspondence for rooted planar maps. *Ars Combin*, 9:11–28, 1980.

[Yea17]   K. Yeats. *A Combinatorial Perspective on Quantum Field Theory*. Springer, first edition, 2017.